

**FRACTURE RESISTANCE OF IMPLANT SUPPORTED ALL
CERAMIC ZIRCONIA-LITHIUM DISILICATE CROWN**



NATTANICH BUNYASRESTH

**A THESIS SUBMITTED IN PARTIAL FULFILLMENT
OF THE REQUIREMENTS FOR
THE DEGREE OF MASTER OF SCIENCE
(IMPLANT DENTISTRY)
FACULTY OF GRADUATE STUDIES
MAHIDOL UNIVERSITY
2016**

Copyright by Mahidol University

COPYRIGHT OF MAHIDOL UNIVERSITY

Thesis
entitled
**FRACTURE RESISTANCE OF IMPLANT SUPPORTED ALL
CERAMIC ZIRCONIA-LITHIUM DISILICATE CROWN**

Nattanich Bunyasresth
.....
Miss Nattanich Bunyasresth
Candidate

S. Somsak Chitmongkolsuk
.....
Assoc. Prof. Somsak Chitmongkolsuk,
Dr. Med. Dent (Prosthodontics)
Major advisor

Widchaya Kanchanavasita
.....
Assoc. Prof. Widchaya Kanchanavasita,
Ph.D. (Biomaterials)
Co-advisor

Patcharee Lertrit
.....
Prof. Patcharee Lertrit,
M.D., Ph.D. (Biochemistry)
Dean
Faculty of Graduate Studies
Mahidol University

Sirichai Kiattavornchareon
.....
Assist. Prof. Sirichai Kiattavornchareon,
M.D., Dip. Thai Board of Oral and
Maxillofacial Surgery
Program Director
Master of Science Program in
Implant Dentistry
Faculty of Dentistry, Mahidol University

Thesis
entitled
**FRACTURE RESISTANCE OF IMPLANT SUPPORTED ALL
CERAMIC ZIRCONIA-LITHIUM DISILICATE CROWN**

was submitted to the Faculty of Graduate Studies, Mahidol University
for the degree of Master of Science (Implant Dentistry)

on
January 18, 2016

Nattanich Bunyasresth

Miss Nattanich Bunyasresth
Candidate

Suthasinee Kasemsarn

Ms. Suthasinee Kasemsarn,
Ph.D., Dip. Thai Board of
Prosthodontics
Chair

Widchaya Kanchanavasita
Assoc. Prof. Widchaya Kanchanavasita,
Ph.D. (Biomaterials)
Member

Somsak Chitmongkolsuk
Assoc. Prof. Somsak Chitmongkolsuk,
Dr. Med. Dent (Prosthodontics)
Member

Patcharee Lertrit
Prof. Patcharee Lertrit,
M.D., Ph.D. (Biochemistry)
Dean
Faculty of Graduate Studies
Mahidol University

Passiri Nisalak
Assoc. Prof. Passiri Nisalak,
B.Sc., D.D.S., M.S. (Orthodontics)
Dip. Thai Board of Orthodontics
Dean
Faculty of Dentistry
Mahidol University

ACKNOWLEDGEMENTS

This thesis has been completed with the support and contribution of many people. I would like to express and pay deeply thanks to my advisor and co advisor, Dr. Somsak Chitmongkolsuk and Dr. Widchaya Kanchanavasita, for many invaluable advices, great support and meaningful guidance they have given me with his skillful knowledge and experience.

I would also like to extend my sincere thanks to Mr. Nopparat Thongpan for his professional assistance and great support to prepare the crowns, Ivoclar Vivadent Company for material supports, Sainamtip Dental Laboratory for fabrication the replica abutments and Research Unit of faculty of dentistry at Chulalongkon University for allowing us to use the research laboratory facilities.

Special thanks to Mr. Kunga Penjor for being excellent buddy and all my master program colleagues for their lovely friendships and support along my study.

Finally, I most gratefully acknowledge my parents and my family for all their support throughout the period of this research.

Nattanich Bunyasresth

**FRACTURE RESISTANCE OF IMPLANT SUPPORTED ALL CERAMIC
ZIRCONIA-LITHIUM DISILICATE CROWN****NATTANICH BUNYASRESTH 5636054 DTIM/M****M.Sc. (IMPLANT DENTISTRY)****THESIS ADVISORY COMMITTEE: SOMSAK CHITMONGKOLSUK, Dr. Med.
Dent, WIDCHAYA KANCHANAVASITA, Ph.D.****ABSTRACT**

The objective of this study was to evaluate the effects of different veneering methods and the effects of different sizes of abutment on the fracture resistance of the crowns and to assess the mode of failure of these crowns.

108 implant abutments were divided into 3 groups with different sizes of abutments [$\text{\O}4.5(\text{s})$, $\text{\O}5.5(\text{m})$ and $\text{\O}6.5(\text{l})$]. Each group of implant abutments contained 3 subgroups of 12 specimens each ($n=12$). A zirconia framework were fabricated on all implant abutments. Various veneering materials were then applied and processed on the zirconia framework. Fluorapatite veneering ceramics were used as the control group (ZAC). Lithium disilicate crowns were fabricated as the veneering layer on the zirconia framework with different procedures: group A bonded via fired Crystal/Connect glass ceramic (FCC) and group B bonded via resin cement (BRC). Resin cement was used for cementation. All specimens were placed in a thermocycling unit and tested with a universal testing machine. Statistical analysis was performed using two-way ANOVA and Tukey B test.

The mean of fracture resistance in the ZAC group was at the highest value (1787-3295N) of cohesive failure. The mean fracture resistance of the FCC group (1714-2809N) was higher than that of the BRC group (1565-1809N). The mean fracture resistance of the abutment diameter 5.5 mm (m) was at the highest value. The largest size of abutment (l) had a mean fracture resistance higher than the smallest size of abutment (s). The two main factors, veneering method and abutment size, had individual effects on fracture resistance. There were significant differences of fracture resistance in all groups with different veneering methods and different sizes of abutment. Adhesive failure was found in the BRC group. Meanwhile the FRC group was found to have both adhesive and combination failure.

The mean fracture resistance of crowns fused with Crystal/Connect was significantly higher than that of crowns bonded with resin cement, but all the crowns had adequate fracture resistance to be used as implant supported restorations in the posterior region.

**KEY WORDS: FRACTURE RESISTANCE / LITHIUM DISILICATE / ZIRCONIA /
VENEERING METHOD / SIZE OF ABUTMENT**

ความทนทานต่อการแตกหักของครอบฟันเซอร่าโคเนีย-ลิเทียมไดซิลิเกตบนรากฟันเทียม

FRACTURE RESISTANCE OF IMPLANT SUPPORTED ALL CERAMIC ZIRCONIA-LITHIUM DISILICATE CROWN

ณัฐนิช บุญยเศรษฐ 5636054 DTIM/M

วท.ม. (ทันตกรรมรากเทียม)

คณะกรรมการที่ปรึกษาวิทยานิพนธ์: สมศักดิ์ จิตรมงคลสุข, Dr. Med. Dent, วิชาญ กาญจนะวสิต, Pd.D

บทคัดย่อ

วัตถุประสงค์ : เพื่อประเมินความทนทานต่อการแตกหักของครอบฟัน โดยใช้กรรมวิธีในการยึดส่วนของผิวครอบฟันด้านนอกต่างกัน และใช้แกนรากฟันเทียมขนาดต่างกัน และเพื่อประเมินลักษณะการแตกหักของครอบฟัน

วัสดุและวิธีการทดลอง : แกนรากฟันเทียม 108 ชิ้น แบ่งเป็น 3 กลุ่มตามขนาดเส้นผ่านศูนย์กลางที่แตกต่างกันของแกนรากฟันเทียม (ขนาดเล็ก 4.5 มม., ขนาดกลาง 5.5 มม., ขนาดใหญ่ 6.5 มม.) และแบ่งเป็นกลุ่มย่อย 3 กลุ่มจำนวนกลุ่มละ 12 ชิ้น โครงเซอร่าโคเนียถูกขึ้นรูปบนแกนรากฟันเทียม ซึ่งมีผิวครอบฟันด้านนอกแตกต่างกันตามชนิดของวัสดุ ได้แก่ กลุ่มเซรามิก (ซีแรม), กลุ่มลิเทียมไดซิลิเกตที่ยึดด้วยคริสตัล/คอนเนค และกลุ่มลิเทียมไดซิลิเกตที่ยึดด้วยเรซินซีเมนต์ ครอบฟันทั้งหมดถูกยึดกับแกนรากฟันเทียมด้วยเรซินซีเมนต์ และนำไปแช่ในเครื่องจำลองอุณหภูมิในช่องปากก่อนนำไปทดสอบด้วยเครื่องวัดแรงอัด ค่าความทนทานต่อการแตกหักของครอบฟันถูกนำมาวิเคราะห์ทางสถิติโดยใช้ความแปรปรวนแบบสองทาง และเปรียบเทียบความแตกต่างโดยวิธีของทูกี

ผลการทดลอง : กลุ่มที่มีค่าเฉลี่ยของความทนทานต่อการแตกหักมากที่สุด คือ กลุ่มซีแรม (1787-3295 นิวตัน) และมีลักษณะรอยแตกอยู่ในผิวครอบฟันด้านนอก ส่วนกลุ่มลิเทียมไดซิลิเกตที่ยึดด้วยคริสตัล/คอนเนค (1714-2809 นิวตัน) มีค่าเฉลี่ยของความทนทานต่อการแตกหักมากกว่ากลุ่มที่ยึดด้วยเรซินซีเมนต์ (1565-1809 นิวตัน) แกนรากฟันเทียมขนาดกลาง 5.5 มม. มีค่าเฉลี่ยของความทนทานต่อการแตกหักมากที่สุด รองลงมาเป็นขนาดใหญ่ 6.5 มม. และขนาดเล็ก 4.5 มม. โดยลำดับ ซึ่งมีความแตกต่างกันอย่างมีนัยสำคัญทางสถิติในทุกกลุ่ม ในกลุ่มลิเทียมไดซิลิเกตที่ยึดด้วยเรซินซีเมนต์ พบลักษณะรอยแตกในส่วนของรอยต่อระหว่างผิวครอบฟันด้านนอกและ โครงเซอร่าโคเนีย ขณะที่ในกลุ่มที่ยึดด้วยคริสตัล/คอนเนค พบลักษณะรอยแตกทั้งในส่วนของรอยต่อระหว่างผิวครอบฟันด้านนอกและ โครงเซอร่าโคเนีย กับรอยแตกของครอบฟันถึงโครงเซอร่าโคเนียทั้งสิ้น

สรุปผลการทดลอง : ค่าเฉลี่ยของความทนทานต่อการแตกหักในกลุ่มลิเทียมไดซิลิเกตที่ยึดด้วยคริสตัล/คอนเนค มีค่ามากกว่ากลุ่มที่ยึดด้วยเรซินซีเมนต์อย่างมีนัยสำคัญทางสถิติ แต่ครอบฟันทุกกลุ่มมีค่าทนทานต่อการแตกหักที่เพียงพอต่อการใช้งานในบริเวณฟันหลัง

CONTENTS

	Page
ACKNOWLEDGEMENTS	iii
ABSTRACT (ENGLISH)	iv
ABSTRACT (THAI)	v
LIST OF TABLES	vii
LIST OF FIGURES	viii
LIST OF ABBREVIATIONS	xi
CHAPTER I INTRODUCTION	1
CHAPTER II LITERATURE REVIEW	3
CHAPTER III MATERIALS AND METHODS	14
CHAPTER IV RESULTS	31
CHAPTER V DISCUSSION	40
CHAPTER VI CONCLUSION	44
REFERENCES	45
APPENDIX	53
BIOGRAPHY	58

LIST OF TABLES

Table	Page
2-1 Properties of LDSC	5
4-1 Mean and standard deviation of fracture resistance (in Newton) of crowns with different designs	31
4-2 Normality test for fracture resistance after removing outliers	32
4-3 Mean and standard deviation of fracture load (in Newton) of crowns with different designs after removing the outliers	33
4-4 Levene's Test of Equality of Error Variances	33
4-5 Analysis of variance	34
4-6 Tukey B Test of fracture resistance in each group of abutment diameter	35
4-7 Tukey B Test of fracture resistance in each group of material types	36
4-8 Mode of failure of crowns with different designs	39
1 Normality test for fracture resistance of crowns	54
2 Normality test for fracture resistance after removing outliers (1 st cut)	55
3 Normality test for fracture resistance after removing outliers (2 nd cut)	56
4 Normality test for fracture resistance after removing outliers (3 rd cut)	57

LIST OF FIGURES

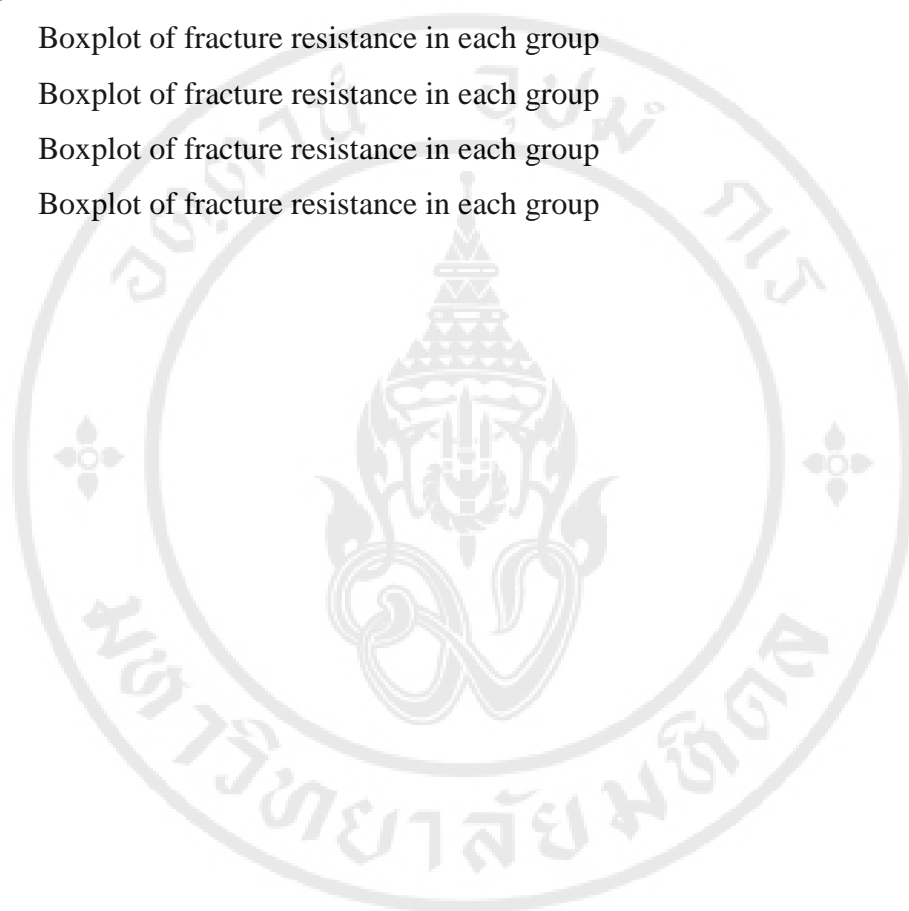
Figure	Page
2-1 A) Monolithic ceramics B) Veneering ceramics with framework	7
2-2 A) Graphics of the fracture pattern distribution B) Visual view of fracture, catastrophic fracture C) Visual view of fracture, chipping	10
2-3 A) Adhesive failure B) Cohesive failure C) Combination failure of adhesive and cohesive failure	12
3-1 Implant abutments ($\varnothing = 4.5$ mm, 5.5 mm and 6.5 mm)	16
3-2 Pattern resin (GC dental, Tokyo, Japan)	16
3-3 Cobalt-Chromium alloy (Vitallium, US)	16
3-4 A) Lithium disilicate glass-ceramic blocks (IPS e.max CAD) B) Zirconium oxide blocks (IPS e.max ZirCAD) C) Fluorapatite veneering ceramic (IPS e.max Ceram) with e.max Ceram build up liquid and Zirliner build up liquid	17
3-5 A) IPS e.max CAD Crystall./Glaze Paste B) IPS e.max CAD Crystall./Connect and Ivomix	17
3-6 CEREC-3 CAD/CAM system (inLab MC XL + inEos Blue)	18
3-7 Programat P300 sintering oven (Ivoclar Vivadent, Liechtenstein))	18
3-8 inFire HTC speed (Sirona, The Dental Company)	18
3-9 Sandblasted machine (Renfert) and Aluminum oxide particles (Al_2O_3)	19
3-10 Ultrasonic cleanser (Q210H, L&R manufacturing, USA)	19
3-11 A) 5% Hydrofluoric acid gel (IPS Ceramic etching gel) B) Monobond N C) Multilink N Self-adhesive resin cement	19
3-12 Epoxy resin (Wilhelm, Germany)	20
3-13 Thermocycling unit (Tc 301, KMIT)	20

LIST OF FIGURES (cont.)

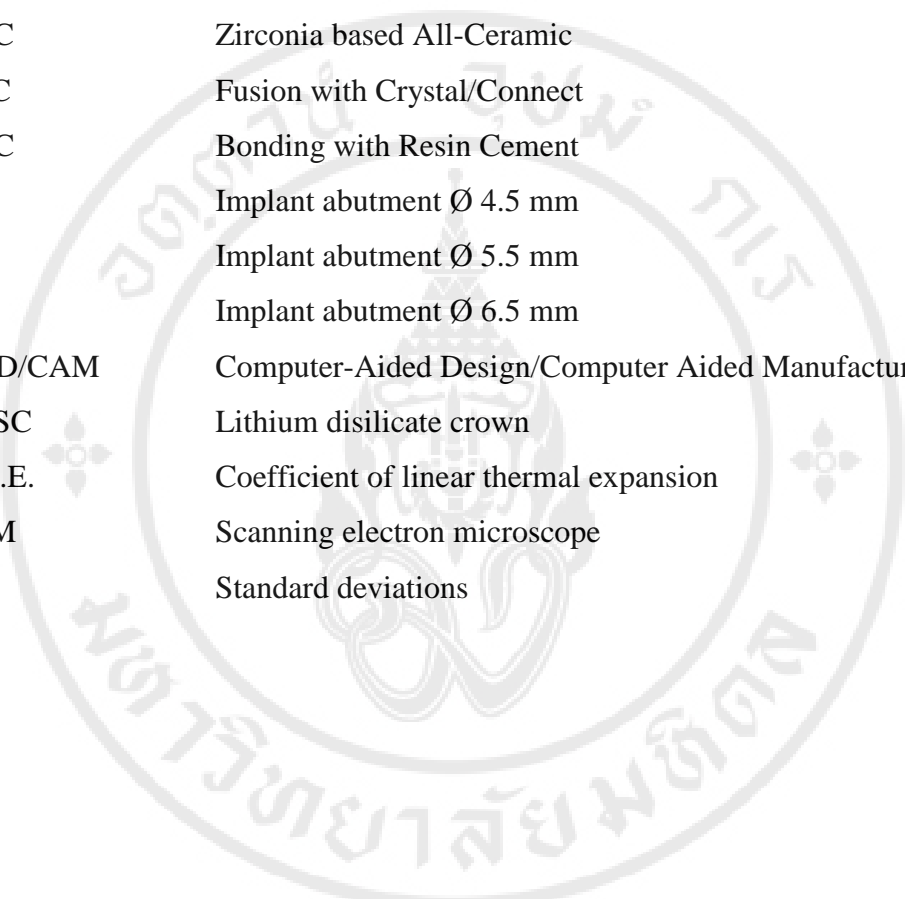
Figure	Page
3-14 Universal testing machine (Instron 8872, UK)	21
3-15 Polarized light microscope (Nikon Eclipse E400 POL, Tokyo, Japan)	21
3-16 Test protocol	23
3-17 Impression mold	24
3-18 Replica abutment	24
3-19 Model for scanning in the CAD process	25
3-20 Standardized dimensions of mandibular first molar	25
3-21 CAD process (framework gap = 60, veneering gap = 40)	26
3-22 ZirCAD framework	26
3-23 Zirconia based all ceramic (ZAC) group, control group	26
3-24 Veneering lithium disilicate crown with glazing after firing in Programat	27
3-25 Sandblasting replica abutment and inner surface of restorative crown	29
3-26 Pre-treatment veneering lithium disilicate crown (Etching with 5% HF gel)	29
3-27 Pre-treatment replica abutment and restorative crown for adhesive bonding technique (Apply Monobond N)	29
3-28 Cementation with Multilink N	30
3-29 The specimen was mounted in steel holder of universal testing machine	30
4-1 Boxplot of fracture resistance of crowns with different designs	32
4-2 Estimated marginal means of fracture resistance in 3 groups of material types	34
4-3 Estimated marginal means of fracture resistance in 3 groups of abutment diameter	35
4-4 Cohesive failure within veneering layer (Control group - ZAC)	37
4-5 Adhesive failure at framework and veneering interface (Test group A - FCC)	38
4-6 Combination of adhesive and cohesive failure (Test group A - FCC)	38
4-7 Adhesive failure at framework and veneering interface (Test group B - BRC)	38

LIST OF FIGURES (cont.)

Figure		Page
1	Boxplot of fracture resistance in each group	54
2	Boxplot of fracture resistance in each group	55
3	Boxplot of fracture resistance in each group	56
4	Boxplot of fracture resistance in each group	57



LIST OF ABBREVIATIONS



ZAC	Zirconia based All-Ceramic
FCC	Fusion with Crystal/Connect
BRC	Bonding with Resin Cement
s	Implant abutment Ø 4.5 mm
m	Implant abutment Ø 5.5 mm
l	Implant abutment Ø 6.5 mm
CAD/CAM	Computer-Aided Design/Computer Aided Manufacturing
LDSC	Lithium disilicate crown
C.T.E.	Coefficient of linear thermal expansion
SEM	Scanning electron microscope
SD	Standard deviations

CHAPTER I

INTRODUCTION

Nowadays dental implants have been widely used as implant therapy for replacing missing teeth. The assessment 10-year outcomes of titanium implants in retrospective study demonstrated a 10-year implant survival rate of 98.8% and a success rate of 97.0%.(1) A systematic review evaluated the incidence of technical complications that can be divided into the major level; such as implant fracture, loss of suprastructures, the medium level; such as abutment fracture, veneer or framework fractures, esthetic and phonetic complications and the minor level; such as abutment and screw loosening, loss of retention, loss of screw hole sealing, veneer chipping and occlusal adjustments. The most common technical complications by implant-supported reconstructions were fractures of veneer material (acrylic, ceramic and composite), abutment or occlusal screw loosening and loss of retention (fracture of the luting cement). Comparing the rate of ceramic fracture or ceramic chipping, the implant-supported fixed dental prostheses had a significantly higher than the tooth-supported fixed dental prostheses. Although framework fracture of the reconstruction was a rare complication. The implant-supported single crowns had high rate fracture of the crown framework (coping). This technical complication was significantly higher in all-ceramic crowns.(2) Further clinical investigations have shown the long-term outcomes with implant-supported restorations. Ceramic chipping was the most frequent complication and was higher rates of fractures in dentitions with attrition and in fixed dental prostheses when compared with single crowns.(3)

In dentistry, the esthetic expectation has led to development of ceramics for esthetic capability, biocompatibility, color stability, wear resistance and low thermal conductivity. During the past decade, limitations of ceramic properties are brittleness and less resistant to tensile forces, which has limited their use for long time. For all of these limitations of ceramic properties, ceramic is superior esthetic appearance but its mechanical properties is not as well as conventional metal material

in posterior region. However, zirconia has been newly introduced for fabrication of restorations in prosthetic dentistry with CAD/CAM techniques. The fracture resistance of zirconia was about twice as high compared to alumina.(4-7) Zirconia showed better mechanical properties and superior resistance to fracture than other conventional dental ceramics but the use of monolithic zirconia fixed dental prostheses is the possible abrasiveness of the material toward enamel. Thus, it has been an alternative framework for fixed dental prostheses. Lithium disilicate was used to be veneering material with various methods to bond between veneer and zirconia framework.(8, 9) Furthermore, Stimmelmayer et al. reported that the fracture strength of the implant abutment increased with the implant diameter.(10)

The aim of this in vitro study were to evaluate the effect of different veneering method and the effect of different abutment size on the fracture resistance of the all ceramic zirconia-lithium disilicate crowns and to assess the mode of failure of these crowns. It was hypothesized that there were no difference in fracture resistance and mode of failure of different veneering method and different abutment size of implant supported all ceramic zirconia-lithium disilicate crowns.

Objectives

To evaluate the effect of different veneering method on the fracture resistance of the all ceramic zirconia-lithium disilicate crowns.

To evaluate the effect of different abutment size on the fracture resistance of the all ceramic zirconia-lithium disilicate crowns.

To assess the mode of failure of these crowns.

Hypothesis

There were no difference in fracture resistance and mode of failure of different veneering method and different abutment size of implant supported all ceramic zirconia-lithium disilicate crowns.

CHAPTER II

LITERATURE REVIEW

2.1 Dental ceramics

Dental ceramics are nonmetallic, inorganic structures containing with a crystal and glass phase based on silica structure. They are glassy with short range crystallinity that used widely because of biocompatibility, strength, esthetics and easier customization.(11)

Dental porcelain has been known in dentistry for hundred years. Esthetics is the main benefit of porcelain, but brittleness property is the weakest point for load-bearing restorations. The conventional powder build-up and firing process is very sensitive technique. In the past, dental ceramic such as glass ceramics, polycrystalline alumina, and zirconia-based ceramics have been used in the clinic with new processing technology, computer-assisted fabrication systems [dental computer-assisted design / computer-assisted manufacturing (CAD/CAM)].

All-ceramic fixed denture prostheses systems have two main types. The first system uses a single material for full crowns. Reinforced glassy materials were used to make single crowns for anterior and premolar regions. Lately, polycrystalline zirconia with improved translucency has been used for full crowns in the molar region. The second system will be fused esthetic ceramics, such as porcelain and other glassy materials, to high-strength ceramic frameworks.(9)

Classification of dental ceramics

1. Microstructural classification

Category 1: Glass-based systems (mainly silica)

Category 2: Glass-based systems (mainly silica) with fillers crystalline

a) Low-to-moderate leucite-containing feldspathic glass

b) High-leucite (~50%) containing glass, glass-ceramics (IPS

Empress)

c) Lithium disilicate glass-ceramics (IPS e.max, pressable and machinable ceramics)

Category 3: Crystalline-based systems with glass fillers (mainly alumina)

Category 4: Polycrystalline solids (alumina and zirconia)

2. Based on processing technique

a) Powder/liquid glass-based systems

b) Pressable blocks of glass-based systems

c) CAD/CAM systems

3. Based on reinforcing method

a) Reinforced ceramic core systems

b) Resin-bonded ceramics

c) Metal-ceramics(11)

2.2 Lithium disilicate (LDSC)

2.2.1 Material properties

Lithium disilicate glass ceramic ($\text{Li}_2\text{Si}_2\text{O}_5$) is one such all-ceramic system, currently used in the fabrication of single and multiunit dental restorations mainly for dental crowns, bridges, and veneers because of its color being similar to natural teeth and its excellent mechanical properties.(12) It was firstly classified as glass-ceramic material by Stookey.(13) Lithium disilicate glass-ceramic was developed by Beall.(14), Freiman and Hench(15) in multicomponent glass systems. Later, the structure of lithium disilicate glass and its corresponding crystal were well known and have been studied for a number of years.(16, 17)

The main properties of LDSC as framework and veneering materials are showed in Table 1. A mechanical property of LDSC as framework material, the average flexural strength of the LDSC after pressing was 400 ± 40 MPa. For the fracture toughness, the KIC value was expressed as 3.3 ± 0.3 MPa \cdot m^{0.5}. Optical properties are very important to the application of glass-ceramics as materials for dental restorations. The very strong and tough LDSC also presented a very good translucency. The contrast ratio value of 0.55 (0 = 100% transparent, 1 = 100%

opaque, disc strength: 1 mm) characterizes this property as being comparable to leucite glass-ceramics and natural dentition. Because of the chemical nature and the microstructure of LDSC, the coefficient of linear thermal expansion (C.T.E.) is $10.6 \pm 0.25 \cdot 10^{-6} \text{ K}^{-1}$ (100–400°C). A favorable property of LDSC is its chemical durability. The characteristic values after treating with acetic acid are less than $50 \mu\text{g}/\text{cm}^2$.

The properties of the layered glass-ceramics (veneering material) are favorable in the optical properties. This material allows the translucency of natural teeth to be matched in dentin and incisal structures. The determined contrast ratio values of the dentin are 0.46. The mechanical strength was established as flexural strength of 80 ± 25 . The C.T.E. value measured $9.7 \pm 0.25 \cdot 10^{-6} \text{ K}^{-1}$ (100–400°C). This material is characterized by very good chemical durability, which is beneficial for dental veneering. The determined parameter is less than $20 \mu\text{g}/\text{cm}^2$.(18)

Table 2-1: Properties of LDSC(18)

Properties	Framework material	Veneering material	Number of samples
Mechanical: • Flexural strength	$400 \pm 40 \text{ MPa}$	$80 \pm 25 \text{ MPa}$	10
Optical: • Translucency	0.55	0.46	1
Thermal • C.T.E.	$10.6 \pm 0.25 \cdot 10^{-6} \text{ K}^{-1}$ (100-400 °C)	$9.7 \pm 0.25 \cdot 10^{-6} \text{ K}^{-1}$ (100-400 °C)	10
Chemical: • Durability	$50 \mu\text{g}/\text{cm}^2$	$20 \mu\text{g}/\text{cm}^2$	8

2.2.2 Processing and reinforcing

LDSC contains two solid phases: the amorphous phase and the crystal phase. The crystal phase of LDSC ($\text{Li}_2\text{Si}_2\text{O}_5$) melts harmoniously at 1033°C and has a stoichiometric composition. This material has the excellent mechanical properties due to the structure of orthorhombic crystals that contains corrugated sheets of $(\text{Si}_2\text{O}_5)^{2-}$ on the (0 1 0) plane.(19) The LDSC was developed recently in the $\text{Li}_2\text{O}-\text{SiO}_2-\text{Al}_2\text{O}_3-\text{K}_2\text{O}-\text{P}_2\text{O}_5$ system to produce high strength of dental restorations in a mechanical shaping process of CAD-CAM technology. It was produced to the method of controlled nucleation and crystallization of the base glasses through heat

treatment.(20) The strength values of ~ 740 MPa (biaxial) in translucent glass-ceramics were achieved by controlling the crystallization mechanism of Li_2SiO_3 and $\text{Li}_2\text{Si}_2\text{O}_5$. A base glass in the $\text{Li}_2\text{O}-\text{SiO}_2-\text{Al}_2\text{O}_3-\text{K}_2\text{O}-\text{P}_2\text{O}_5$ system was added ZrO_2 to be nucleating agent. The reaction of ZrO_2 as a nucleating agent was first presented by Tashiro and Wada(21) and later by Beall(14). The present study of Apel et al. found that ZrO_2 influences the reaction kinetics of the crystallization processes of both lithium metasilicate and lithium disilicate. The ZrO_2 -free glass-ceramic has a very fine and strong microstructure. With the increasing ZrO_2 content, the crystals become smaller. It increases in the viscosity property and the linked reduction in crystal growth of Li_2SiO_3 and $\text{Li}_2\text{Si}_2\text{O}_5$. The strength values are lower than in the base glass. By increasing the crystallization temperature the crystal growth could be improved with higher strength. The translucency of LDSC is adjusted by adding ZrO_2 .(22)

2.2.3 Types of LDSC - classification

LCDS can be classified either according to processing technique into hot pressing techniques and CAD-CAM milling procedures, or based on application into monolithic ceramics and veneering ceramics with a framework.

2.2.3.1 Hot pressing techniques

Pressable ceramic ingots are fabricated by the lost-wax technique. They contain crystalline particles that have the microstructure same as powder porcelains. However, pressable ceramics have less porosity and higher crystalline content due to transformation of the glass into crystals in heat process of manufactured ingots. In laboratory process, these ingots are heated to a temperature with highly viscous liquid and slowly pressed into the lost wax mold.(23) The higher crystalline content and lack of porosity do not effect to fracture resistance.(24) But the benefit of this method, hot pressing, is good accuracy of fit with metal alloys.(25, 26)

2.2.3.2 CAD-CAM milling procedures

CAD/CAM ceramic ingots are fabricated by using computer-controlled tools. The presintered ingots with porous are fast milled without bulk fracture of the ceramic but it need to eliminate the porosity by sintering treatment. The computer software is good accuracy of fit due to compensating for the shrinkage.

However, if the presintered ingots are sintered before milling process, it can improve the disadvantage of the shrinkage that occurs during sintering process. But densely sintered ceramic with non-porous ingots are more difficult to mill. Glass infiltrated CAD/CAM ingots have same composition to slip cast ceramic, but it starts with a porous ingot to reduce the complicated process of slip casting. The porosity is eliminated after milling by molten glass infiltration.(23) There is one of the question about surface cracks that occur during milling process are weaken CAD/CAM ceramics in densely sintered ingots, but there is no evidence in the current literature of this effect.(27)

2.2.3.3 Monolithic ceramics

Monolithic ceramic (see Fig. 1A) was introduced by using LDSC such as IPS e.max Press and IPS e.max CAD. It has two forms: a homogeneous ingot with hot-pressed technique and a precrystallized block with CAD/CAM technique. Both forms can be fabricated a full anatomical contour with the application of stain and glaze or a cut-back and layering technique.(28)

2.2.3.4 Veneering ceramics with framework

Bi-layered crown systems are supported by a framework or substructure core (see Fig. 1B). Various materials are used to fabricate substructure such as metal alloy, alumina, and zirconia.(28) Ceramo-metal crowns are used frequently due to the strength, biocompatibility, and esthetics.(29) However, the use of nonmetallic with high strength core materials has increased because patients demand more esthetics. The esthetic core materials include alumina, zirconia, and lithium disilicate. Veneering porcelains are made to fabricate core to create the final restorations.(30, 31)



Fig. 2-1: A: Monolithic ceramics. B: Veneering ceramics with framework (Source: R&D Ivoclar Vivadent)

2.3 Zirconia

Zirconia is the dental ceramics, which pure form of zirconia is a polymorphic crystal. Three different crystalline phases relate to temperature: monoclinic (room temperature until 1170°C, tetragonal (1170-2370°C) and cubic (2370 until melting point 2380°C). Stabilizers, yttrium and cerium oxide, are added to prevent phase transformation and retain tetragonal phase of zirconia more stable at room temperature. Yttria-stabilized tetragonal zirconia polycrystal (Y-TZP) was called with higher mechanical properties than other ceramics.(4, 6)

When a crack initiates on the surface of zirconia, the stress concentration causes the transformation of a tetragonal crystal into a monoclinic crystal, with volumetric expansion. Micro-structural defects within zirconia material cause cracks in combination with tensile forces. Increasing fracture toughness will slow down crack propagation and has effect on long-term stability of material. In the vicinity of a progressive crack, the stress-induced transformation leads to compressive stress and enhances the fracture toughness.(7, 9)

CAD/CAM technology has scanned the prepared abutment and designed framework before milling by using computer software. Two types of zirconia milling processes are available:

- 1) Soft-milling associates machining enlarged frameworks out of pre-sintered blanks of zirconia, also called the “green” state and sintering to their full strength. It has shrinkage of the milled framework approximate 25%.

- 2) Hard-milling associates machining the framework directly to the dimension out of densely sintered (higher strength and more homogenous) zirconia blanks with hot isostatic pressed (HIPed).

For weak points of soft and hard milling, hard-milling may have microcracks in the framework during the milling process. On the other hand, soft-milling has less marginal fit when compare to hard-milling because there is shrinkage in soft-milling process.(4)

Veneering ceramics were fabricated on zirconia framework involves esthetics and harmonized to natural teeth. There are various methods of bonding between veneering ceramics and zirconia.

1) The layering technique, porcelain powder is applied onto the zirconia framework before firing. The outcome of this technique is excellent esthetics, but several firings are needed to reproduce the desired color and shape.

2) The press technique, the lost wax technique is used to create the restoration. A homogeneous ceramic ingot is heated and forced under pressure into a wax-formed void. This technique is easy shaping but it is hard to reproduce the desired color because of the ceramic ingot. Thus, the outcome of this technique has only a single color.

For both the layering technique and the press technique, the coefficient of thermal expansion between zirconia framework and veneering ceramic is important because a large difference in CTE will cause residual stress on the crown and reduce reliability of the restoration.

3) Bonding of zirconia with resin-based luting agents(9)

A clinical complication of zirconia restorations, veneering porcelain fracture is high incidence rate of clinical finding as chipping fractures. Moreover, an intrinsic accelerated aging is problem that occurs in zirconia in a humid environment as low-temperature degradation. This aging phenomenon causes a decrease in strength of zirconia by spontaneous slow phase transformation from the tetragonal phase to the weaker monoclinic phase putting zirconia frameworks at risk of spontaneous catastrophic failure.(4, 5)

2.4 Failure types

Mode of failure can be classified in various categories according to naked eye examination into chipping and catastrophic fracture, or based on examination with optical microscope and scanning electron microscope (SEM) into adhesive failure, cohesive failure, and combination failure.

2.4.1 Category 1 – examination with naked eye

The failure type was estimated after loading with universal testing machine to evaluate the fracture resistance. Mode of failure can be divided into 2 groups as chipping and catastrophic fracture. This failure type can be examined by naked eye, as seen in Fig. 2

2.4.1.1 Group 1: Catastrophic fracture

Catastrophic fractures are most found in monolithic crowns that have a better fracture resistance than veneered crowns.(32) In this fracture, the veneering layer is destroyed until the substructure exposed. Veneering or framework fracture is the medium level of technical complication.(2)

2.4.1.2 Group 2: Chipping

Chipping is most likely to occur at lower occlusal loads because of a stage of stable crack propagation prior to final spallation catastrophic.(33) The crack deflection is effect on the superior resistance of substructure.(32) In this fracture, the fracture occurs in veneering layer. Thus, it is divided into the minor level of technical complication.(2)

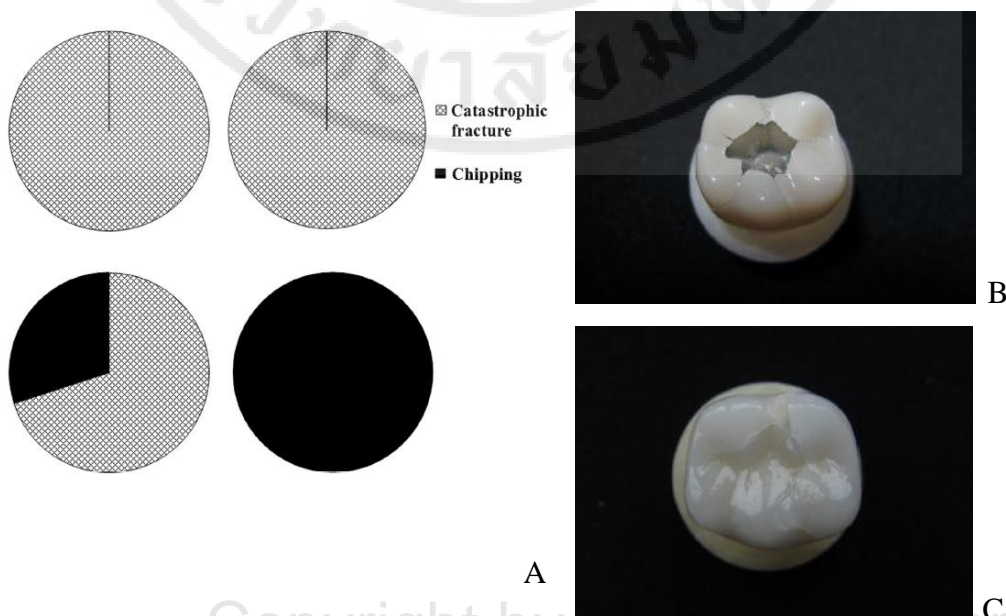


Fig. 2-2: A) Graphics of the fracture pattern distribution. B) Visual view of fracture, catastrophic fracture. C) Visual view of fracture, chipping(32)

2.4.2 Category 2 – examination with microscope

Evaluation of the failure type is examined by using optical microscope and SEM. The failure mode can be classified into 3 groups as adhesive failure, cohesive failure, and combination failure.

2.4.2.1 Group 1: Adhesive failure

Adhesive failure occurs at framework and veneering interface. It always causes complete delamination of the veneer ceramic from the framework.(34, 35) For monolithic LDSC, the failure mode is bulk fracture of the substructure and veneering porcelain.(36) The horizontal crack is parallel to the interface and longer than the vertical.(37) Adhesive failure, as seen in Fig. 3A, is found beside a void. Wake hackles (white arrows) indicate the crack starts near the void (white star).(38)

2.4.2.2 Group 2: Cohesive failure

Cohesive failure is the critical cracks initiate from occlusal fissures. It is the chip-off fracture limited within veneering layers. A thin layer of porcelain that remains on the framework is associated with this failure.(34, 35) The characteristic of cohesive failure, as seen in Fig. 3B, is a typical brittle fracture that originates from the occlusal surface of veneering ceramic. Circumferential patterns on the fracture surface (white arrow) indicate the pattern of crack growth, intersection and extension through the substructure.(38)

2.4.2.3 Group 3: Combination of adhesive and cohesive failure

In this failure type, it found both failure at interface between framework and veneering including within veneering layer. Adhesive and cohesive failure is bulk of veneering ceramic fractured from framework to expose the substructure while residual veneer porcelain still remains. Combination failure is showed in Fig. 3C. A crack goes parallel to the veneer-substructure interface, but still locates within veneering layer (white arrow). A step-like fracture surface in front of the crack is formed and framework is partially exposed.(38)

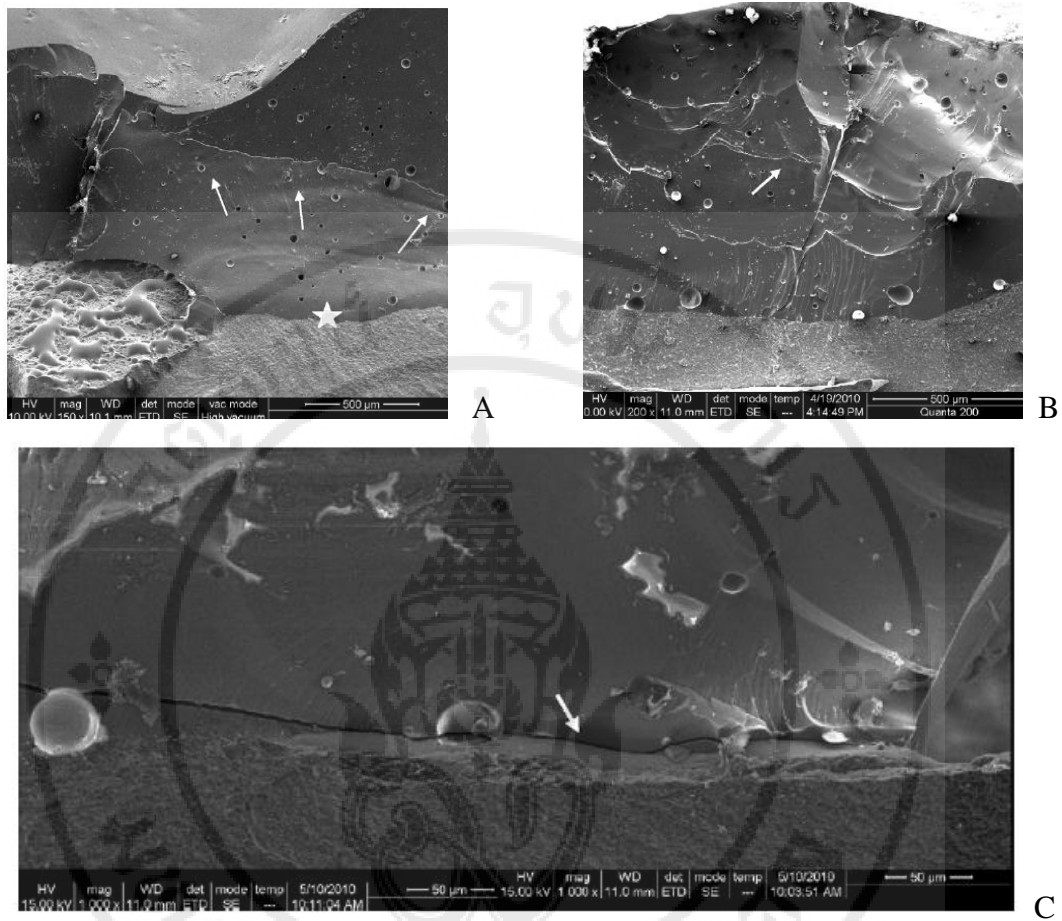


Fig. 2-3: A) Adhesive failure. B) Cohesive failure. C) Combination failure of adhesive and cohesive failure.(38)

2.5 The fracture loads and failure types of LDSC

In the testing of fracture resistance, the loading is evaluated by using the testing machine. The maximum loading is recorded when the prosthesis is fractured and the testing machine is stopped. This maximum loading is the failure loading or fracture resistance of prosthesis. After that, the failure type is examined by naked eye and microscope to classify the mode of failure.

The fracture loads and failure type of LDSC are presented in table 2. Sun et al. showed the fracture load and fracture mode of monolithic LDSC (IPS e.max Press). All single crowns were fabricated in full anatomy of mandibular first molar with 1.5 mm occlusal thickness and tested in static loading by using the universal

testing machine. The mean fracture load was 1863.16 ± 116.81 N and the fracture mode was catastrophic fracture.(32) Furthermore, the study of Dhima et al. found the mean static failure load of the monolithic LDSC in a wet environment was 743.1 ± 114.3 N.(39) It was still higher than average posterior masticatory forces (150-340 N).(40) Hertzian cracks were the mode of failure surrounding the contact zone, the sloped surface were a more radial crack propagation pattern.(39)

For bi-layered crowns or veneering ceramics with framework, LDSC were used as the core materials (IPS e.max Press) with the veneer (IPS e.max Ceram). All flat bi-layered specimens (core thickness 0.8 mm with veneer thickness 1.2 mm) were tested in static loading and cyclic loading. The mean compressive load to fracture in static loading was 857 ± 66 N. After cyclic loading, the mean compressive load was reduced from 857 to 645 N. However, the adhesive failure, the horizontal crack was parallel to the interface of the core and veneer, could be found in both groups of static loading and cyclic loading.(37)

To compare between monolithic and bi-layered crowns, the monolithic LDSC showed superior performance more than bi-layered LDSC. The mean fracture load values of monolithic crowns before fatigue and after fatigue were 2686 ± 628 N and 2133 ± 578 N, respectively. Whereas, the mean fracture load values of bi-layered crowns before fatigue and after fatigue were 1443 ± 327 N and 1464 ± 419 N, respectively. The mode of failure of these crowns was similar in bulk fracture type, but different in crack propagation from the site of fracture initiation.(41)

On the other hand, LDSC were used as veneering layer (IPS e.max CAD) with zirconia framework (IPS e.max ZirCAD). Attachment techniques between LDSC veneer and zirconia framework were compared. Luting with resin cement (Multilink), the fracture resistance was 1211 ± 158 N (static loading) and 1226 ± 290 N (static loading after chewing simulation and thermal cycling). Adhesive failure between core and resin cement was found in static loading and adhesive failure between veneer and resin cement was found in static loading after chewing simulation and thermal cycling. Veneer fused to framework by using fusion ceramic (IPS e.max Crystall./Connect), the fracture resistance was 1388 ± 190 N (static loading) and 1492 ± 206 N (static loading after chewing simulation and thermal cycling). Combination failure (cohesive and adhesive failure) occurred in fused crowns.(42)

CHAPTER III

MATERIALS AND METHODS

Materials and apparatus

1. Implant abutment (Straight 3.5/4.0 TiDesign™, AstraTech Dental)
(Fig 3-1)
 - 1.1 Ø 4.5, 1.5 mm
 - 1.2 Ø 5.5, 1.5 mm
 - 1.3 Ø 6.5, 1.5 mm
2. Pattern resin (GC dental, Tokyo, Japan) (Fig 3-2)
3. Silicone impression materials (Wiscosil[®], BEGO, Germany)
4. Cobalt-Chromium alloy (Vitallium, US) (Fig 3-3)
5. Lithium disilicate glass-ceramic blocks for the CAD/CAM technique (IPS e.max CAD, Ivoclar Vivadent, Liechtenstein) (Fig 3-4A)
6. Zirconium oxide blocks for the CAD/CAM technique (IPS e.max ZirCAD, Ivoclar Vivadent, Liechtenstein) (Fig 3-4B)
7. Fluorapatite veneering ceramic (IPS e.max Ceram) with IPS e.max Ceram Build-up liquid all around and IPS e.max Ceram Zirliner Build-up liquid all around (Ivoclar Vivadent, Liechtenstein) (Fig 3-4C)
8. IPS e.max CAD Crystall./Glaze Paste (Ivoclar Vivadent, Liechtenstein) (Fig 3-5A)
9. IPS e.max CAD Crystall./Connect (Ivoclar Vivadent, Liechtenstein) and Ivomix (Fig 3-5B)
10. CEREC-3 CAD/CAM system (inLab MC XL + inEos Blue, Sirona) (Fig 3-6)
11. Programat P300 sintering oven (Ivoclar Vivadent, Liechtenstein) (Fig 3-7)
12. inFire HTC speed (Sirona, The Dental Company) (Fig 3-8)

13. Sandblasted machine (Renfert Vario Basic Sandblaster) and Aluminum oxide particles (Al_2O_3) (EDELKORUND/KOROSAN sandblasting material) (Fig 3-9)
14. Ultrasonic cleanser (Q210H, L&R manufacturing, USA) (Fig 3-10)
15. 5% Hydrofluoric acid gel (IPS Ceramic etching gel, Ivoclar Vivadent, Liechtenstein) (Fig 3-11A)
16. Monobond N (Ivoclar Vivadent, Liechtenstein) (Fig 3-11B)
17. Multilink N Self-adhesive resin cement (Ivoclar Vivadent, Liechtenstein) (Fig 3-11C)
18. Epoxy resin (Dr. Wilhelm Kohlhaus GmbH & Co, Aschaffenburg, Germany) (Fig 3-12)
19. PVC rings ($\text{Ø} = 18$ mm, height 25 mm)
20. Tin foil (0.3 mm thick)
21. Thermocycling unit (Tc 301, KMIT. At Chulalongkorn university, Bangkok, Thailand) (Fig 3-13)
22. Universal testing machine (Instron 8872, UK. At Chulalongkorn university, Bangkok, Thailand) (Fig 3-14)
23. Polarized light microscope (Nikon Eclipse E400 POL, Tokyo, Japan) (Fig 3-15)



Fig. 3-1: Implant abutments (Straight 3.5/4.0 TiDesign™, Astra Tech) with 3 emergence profiles ($\text{Ø} = 4.5 \text{ mm}$, 5.5 mm and 6.5 mm)



Fig. 3-2: Pattern resin (GC dental, Tokyo, Japan)



Fig. 3-3: Cobalt-Chromium alloy (Vitalium, US)



Fig. 3-4: A) Lithium disilicate glass-ceramic blocks (IPS e.max CAD)
 B) Zirconium oxide blocks (IPS e.max ZirCAD)
 C) Fluorapatite veneering ceramic (IPS e.max Ceram) with e.max Ceram build up liquid and Zirliner build up liquid



Fig. 3-5: A) IPS e.max CAD Crystall./Glaze Paste
 B) IPS e.max CAD Crystall./Connect and Ivomix



Fig. 3-6: CEREC-3 CAD/CAM system (inLab MC XL + inEos Blue)



Fig. 3-7: Programat P300 sintering oven (Ivoclar Vivadent, Liechtenstein)



Fig. 3-8: inFire HTC speed (Sirona, The Dental Company)



Fig. 3-9: Sandblasted machine (Renfert) and Aluminum oxide particles (Al_2O_3)



Fig. 3-10: Ultrasonic cleanser (Q210H, L&R manufacturing, USA)

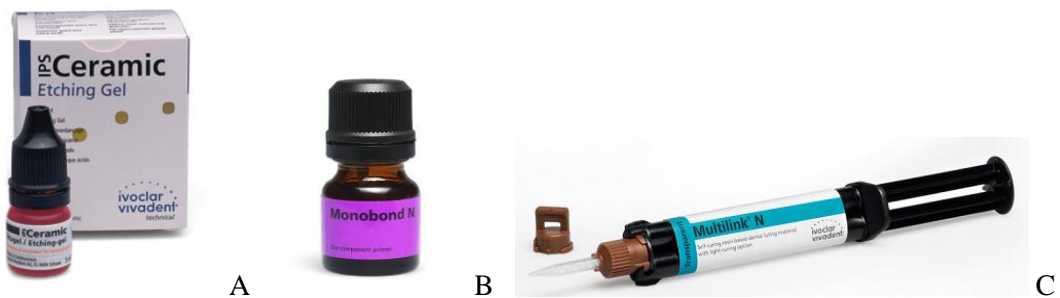


Fig. 3-11: A) 5% Hydrofluoric acid gel (IPS Ceramic etching gel)

B) Monobond N

C) Multilink N Self-adhesive resin cement



Fig. 3-12: Epoxy resin (Wilhelm, Germany)



Fig. 3-13: Thermocycling unit (Tc 301, KMIT)



Fig. 3-14: Universal testing machine (Instron 8872, UK)



Fig. 3-15: Polarized light microscope (Nikon Eclipse E400 POL, Tokyo, Japan)

Methods

A total of 108 implant abutments were used in the in vitro investigation. All implant abutments were divided into 3 groups with different diameter of implant abutments ($\text{\O} = 4.5 \text{ mm}$, 5.5 mm and 6.5 mm). Each group of implant abutments contained 3 subgroups of 12 specimens each ($n=12$). ZirCAD framework (IPS e.max ZirCAD) were fabricated on all implant abutments. Various veneering materials were then applied and processed on the ZirCAD framework. Fluorapatite veneering ceramics (IPS e.max Ceram) were used as the control group (group C). Lithium disilicate crowns (IPS e.max CAD) were fabricated as veneering layer on ZirCAD framework with different procedures; group A bonded via fired Crystal/Connect glass ceramic and group B bonded via resin cement.

Self-curing luting composite (Multilink N) were used to bond the restorative crowns to the replica abutments made from cobalt-chromium alloy. All specimens were embedded in a self-polymerizing resin block (PVC ring $\text{\O} = 18 \text{ mm}$, height 25 mm). 24 hours after cementation, all specimens were placed in the thermocycling unit and tested with universal testing machine.

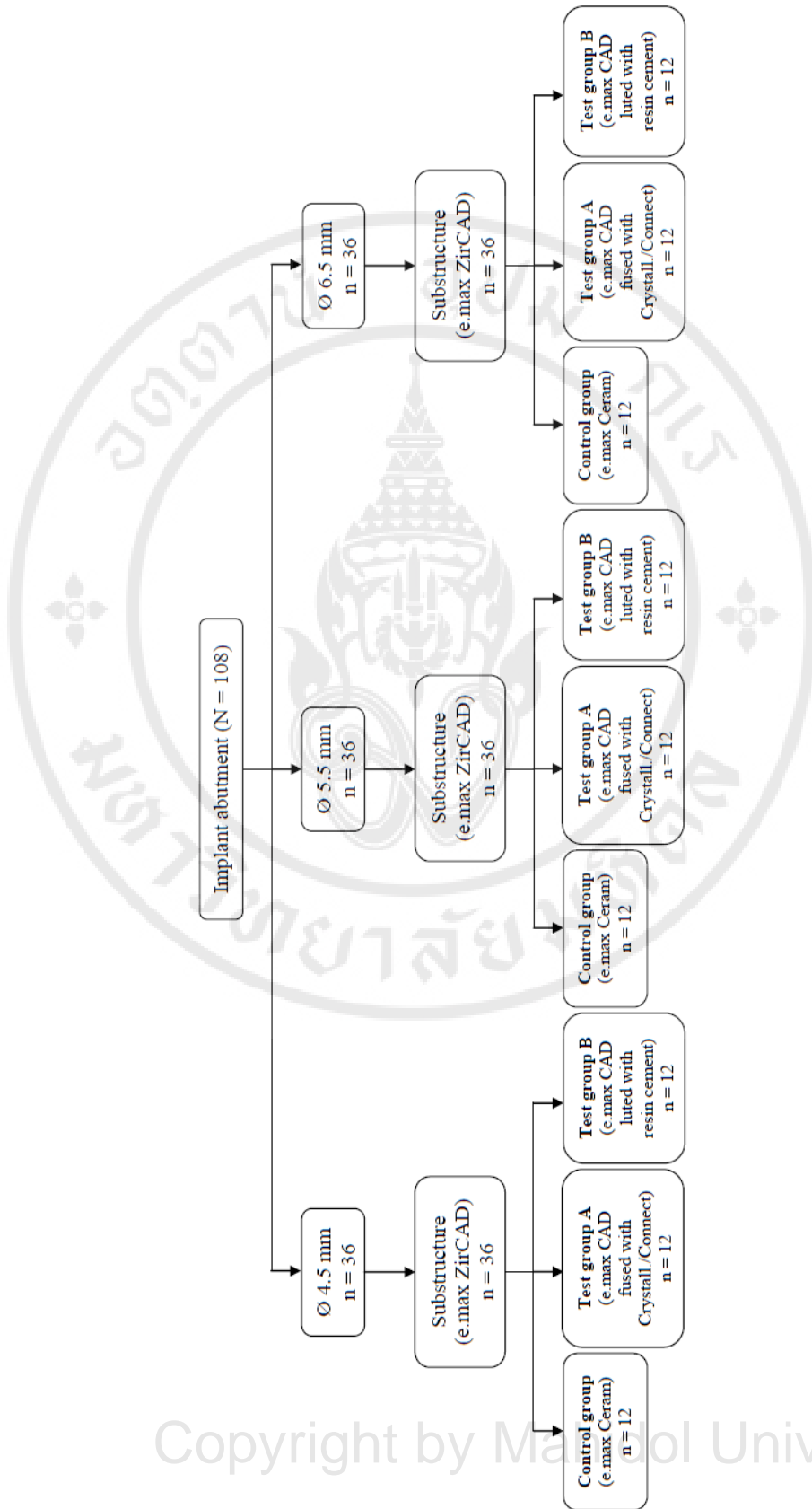


Fig 3-16: Test protocol

3.1 Fabrication of implant abutments

Three implant abutments (Straight 3.5/4.0 TiDesign™, Astra Tech) with 3 emergence profiles ($\varnothing = 4.5, 5.5$ and 6.5 mm) were used as model to fabricate the replica abutments. Each implant abutment ($\varnothing = 4.5, 5.5$ and 6.5 mm) and implant analog were duplicated to construct the impression mold by silicone impression material (Fig. 3-17). Pattern resins were poured to impression mold and putty index was used to connect between abutment part and analog part. After that, they were sent to dental laboratory for casting with cobalt-chromium alloy (Fig. 3-18). A total of 108 implant abutments were used in this study.

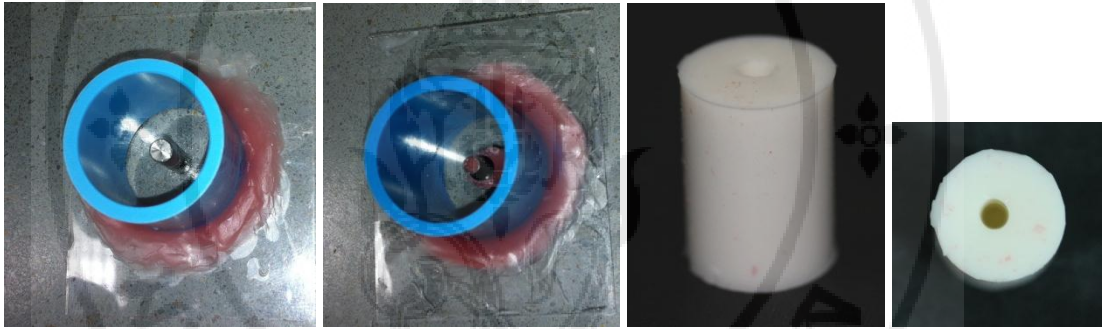


Fig. 3-17: Impression mold



Fig. 3-18: Replica abutment

3.2 Fabrication of restorative crowns

All crowns were controlled in standardized dimensions of mandibular first molar (mesio-distal width = 11.9 mm, bucco-lingual width = 11.1 mm, occlusal thickness at central fossa = 1.5 mm). Restorative frameworks were fabricated using zirconium oxide block for CAD/CAM technique (IPS e.max ZirCAD, Ivoclar Vivadent). Framework fabrication was scanned and milled using CAD/CAM system with minimum framework dimensions of crowns (occlusal thickness at central fossa = 0.5 mm). Substructure was designed in anatomical shape.

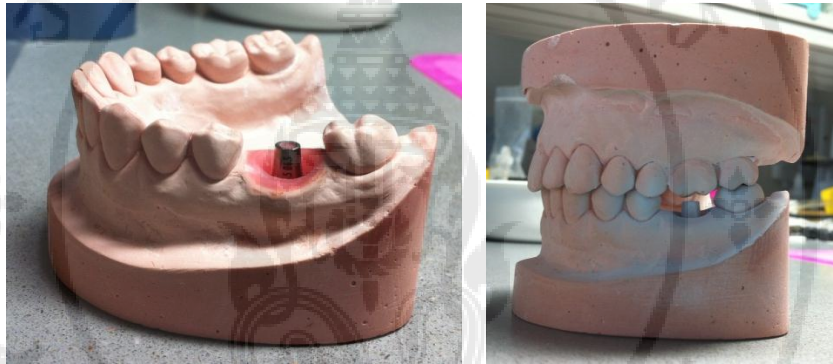


Fig. 3-19: Model for scanning in the CAD process

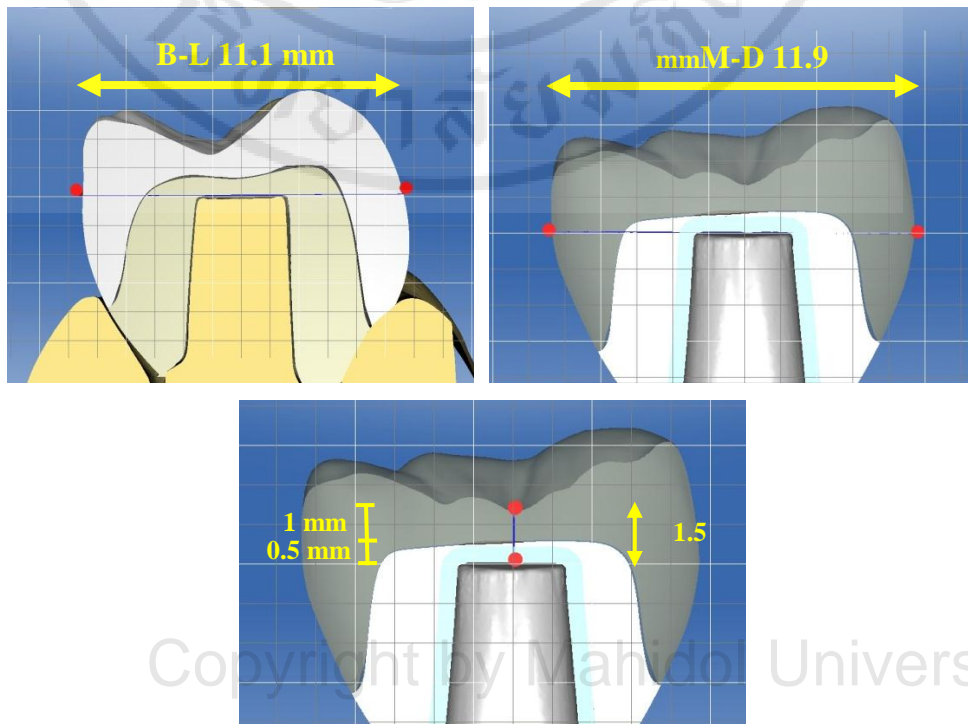


Fig. 3-20: Standardized dimensions of mandibular first molar

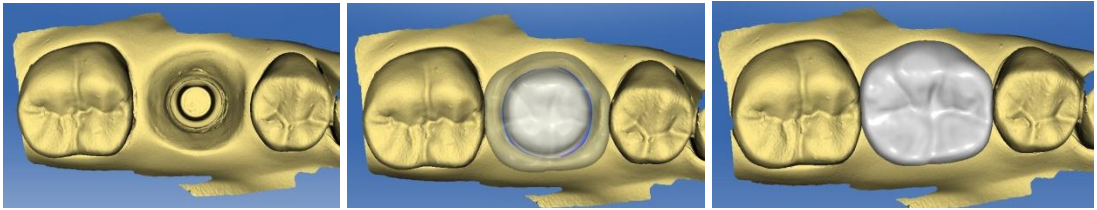


Fig. 3-21: CAD process (framework gap = 60, veneering gap = 40)



Fig. 3-22: ZirCAD framework

Various veneering materials on ZirCAD framework were designed to each group. In control group (n=36), thirty-six ZirCAD frameworks were fabricated veneering layer by firing process of fluorapatite veneering ceramics (Zirconia based all ceramic, ZAC). The crowns were controlled by vacuum form in cast and measured the sizes by vernier calipers (Fig. 3-23).



Fig. 3-23: Zirconia based all ceramic (ZAC) group, control group

In test group, seventy-two ZirCAD frameworks were fabricated veneering layer with lithium disilicate crowns (IPS e.max CAD). Test group A (n=36), thirty-six ZirCAD frameworks were bonded via fired crystal connect glass ceramic (Fusion with Crystal/Connect, FCC). IPS e.max CAD veneering structure was fused to a zirconium oxide framework by means of innovative IPS e.max CAD crystal/connect fusion glass-ceramic. The fusion and crystallization firing was conducted in a Programat. Test group B (n=36), thirty-six ZirCAD frameworks were bonded via resin cement (Bonding with Resin cement, BRC).

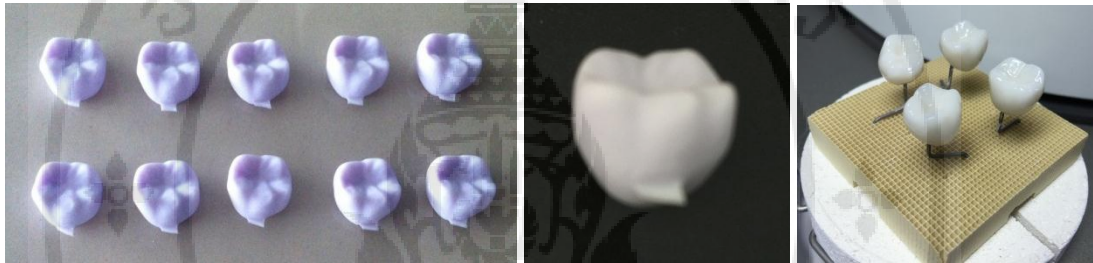


Fig. 3-24: Veneering lithium disilicate crown with glazing after firing in Programat

Material Specifications

IPS e.max ZirCAD (Ceramic blocks for the CAD/CAM technology)

Standard composition:	(in wt %)
ZrO ₂	87.0 – 95.0
Y ₂ O ₃	4.0 – 6.0
HfO ₂	1.0 – 5.0
Al ₂ O ₃	0.0 – 1.0

Physical properties:

CTE (100-400°C) [10 ⁻⁶ /K]	10.8
CTE (100-500°C) [10 ⁻⁶ /K]	10.8
Flexural strength (biaxial) [MPa]*	900
Fracture toughness [MPam ^{0.5}]	5.5
Vickers hardness [MPa]	13000
Chem. solubility [µg/cm ²]*	1
Sinter temperature [°C/°F]	1500/2732

*according to ISO 6872

IPS e.max Ceram

Physical properties:

CTE (100-400°C) [$10^{-6}/K$]	9.5
Flexural resistance (biaxial) [MPa]*	90
Vickers hardness [MPa]	5400
Chem. solubility [$\mu\text{g}/\text{cm}^2$]*	15
Firing temperature [$^{\circ}\text{C}/^{\circ}\text{F}$]	750/1382

*according to ISO 6872

IPS e.max CAD

Physical properties:

CTE (100-400°C) [$10^{-6}/K$]	10.2
CTE (100-500°C) [$10^{-6}/K$]	10.5
Flexural strength (biaxial) [MPa]*	360
Fracture toughness [$\text{MPa}\text{m}^{0.5}$]	2.25
Modulus of elasticity [GPa]	95
Vickers hardness [MPa]	5800
Chem. solubility [$\mu\text{g}/\text{cm}^2$]*	40
Sinter temperature [$^{\circ}\text{C}/^{\circ}\text{F}$]	840–850/1544-1562

*according to ISO 6872

3.3 Cementation

Pre-treatment for adhesive bonding technique: all abutment surface and inner surface of restorative crowns were sandblasted with aluminum oxide (grain size 50 μm at 2 bars), cleaned in ultrasonic cleaner and dried with oil-free compressed air (Fig. 3-25). After that, veneering lithium disilicate crowns were etched with 5% Hydrofluoric acid gel and rinsed with water before cementation to zirconia framework (Fig. 3-26). All replica abutments and restorative crowns were applied Monobond N (Fig. 3-27). The self-curing luting composite (Multilink N) were used to bond the restorative crowns to the replica abutments that made from cobalt-chromium alloy. After positioning of the restoration, pressure was applied to the central occlusal fossa

of the specimen until cement material was cured about 1 minute (Fig. 3-28). All specimens were embedded in a self-polymerizing resin block (PVC ring $\varnothing = 18$ mm, height 25 mm). The platforms of implant abutments are 2.0 mm away from the acrylic resin blocks. After 24 hours of cementation, all specimens were exposed to 10,000 thermal cycles of 5°C and 55°C, with a 30 second dwell-time at each temperature.



Fig. 3-25: Sandblasting replica abutment and inner surface of restorative crown



Fig. 3-26: Pre-treatment veneering lithium disicate crown (Etching with 5% Hydrofluoric acid gel)



Fig. 3-27: Pre-treatment replica abutment and restorative crown for adhesive bonding technique (Apply Monobond N)



Fig. 3-28: Cementation with Multilink N

3.4 Fracture resistance test

The specimen was mounted in steel holder of universal testing machine (Fig. 3-29). To prevent local force concentrations, tin foil was placed between the tip of the punch and the test specimen. The force was applied axially to the occlusal surface of specimen at a 0° degree to simulate posterior tooth contact with 3/16 inches diameter steel ball by using load cell at a consistence crosshead speed of 1.0 mm/min. The crosshead motion was stopped after restorative crown has fractured. The maximum load was recorded. The values of mean and standard deviation of fracture resistance were calculated and recorded in each group of specimens. The effect of different veneering method and the effect of different size of abutment on the fracture resistance of the crowns were analyzed by using two-way ANOVA and Tukey B tests.

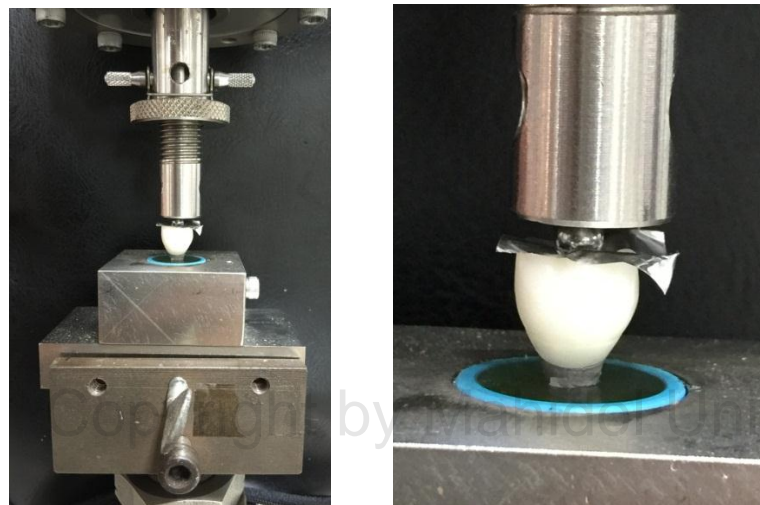


Fig. 3-29: The specimen was mounted in steel holder of universal testing machine

CHAPTER IV RESULTS

After thermocycling 10,000 cycles, fracture resistance of all crowns were determined. Mean and standard deviation in each group are shown in Table 4-1.

Table 4-1: Mean and standard deviation of fracture resistance (in Newton) of crowns with different designs (n=12)

Material types	Abutment diameter	Fracture resistance (N) Mean ± SD	Shapiro-Wilk		
			Statistic	df	Sig.
Zirconia based All-Ceramic (ZAC)	4.5 mm (s)	1985 ± 539	.910	12	.214
	5.5 mm (m)	3295 ± 986	.950	12	.635
	6.5 mm (l)	2851 ± 733	.960	12	.786
Fusion with Crystal/Connect (FCC)	4.5 mm (s)	1714 ± 508	.888	12	.110
	5.5 mm (m)	2809 ± 1073	.949	12	.625
	6.5 mm (l)	2293 ± 788	.913	12	.230
Bonding with Resin Cement (BRC)	4.5 mm (s)	1565 ± 229	.911	12	.220
	5.5 mm (m)	1804 ± 159	.844	12	.031
	6.5 mm (l)	1834 ± 181	.786	12	.007

* **ZAC** = Zirconia based All-Ceramic, **FCC** = Fusion with Crystal/Connect, **BRC** = Bonding with Resin Cement, *s* = Ø 4.5 mm, *m* = Ø 5.5 mm, *l* = Ø 6.5 mm

Data in each group were subjected to normality test using Shapiro-Wilk test, Levene’s test for equality of variances and Boxplot for outliers and extreme values. This was carried out until no outliers were presented, and normally distributed data were obtained, as shown in table 4-2 and fig 4-1. Note that the final sample sizes in each group were not equal.

Table 4-2: Normality test for fracture resistance after removing outliers

	Material types	Abutment diameter	Sample size (n)	Shapiro-Wilk		
				Statistic	df	Sig.
Fracture resistance (N)	Zirconia based All-Ceramic (ZAC)	4.5 mm (s)	10	.951	10	.684
		5.5 mm (m)	12	.950	12	.635
		6.5 mm (l)	12	.960	12	.786
	Fusion with Crystal/Connect (FCC)	4.5 mm (s)	12	.888	12	.110
		5.5 mm (m)	12	.949	12	.625
		6.5 mm (l)	12	.913	12	.230
	Bonding with Resin Cement (BRC)	4.5 mm (s)	12	.911	12	.220
		5.5 mm (m)	8	.874	8	.165
		6.5 mm (l)	11	.963	11	.807

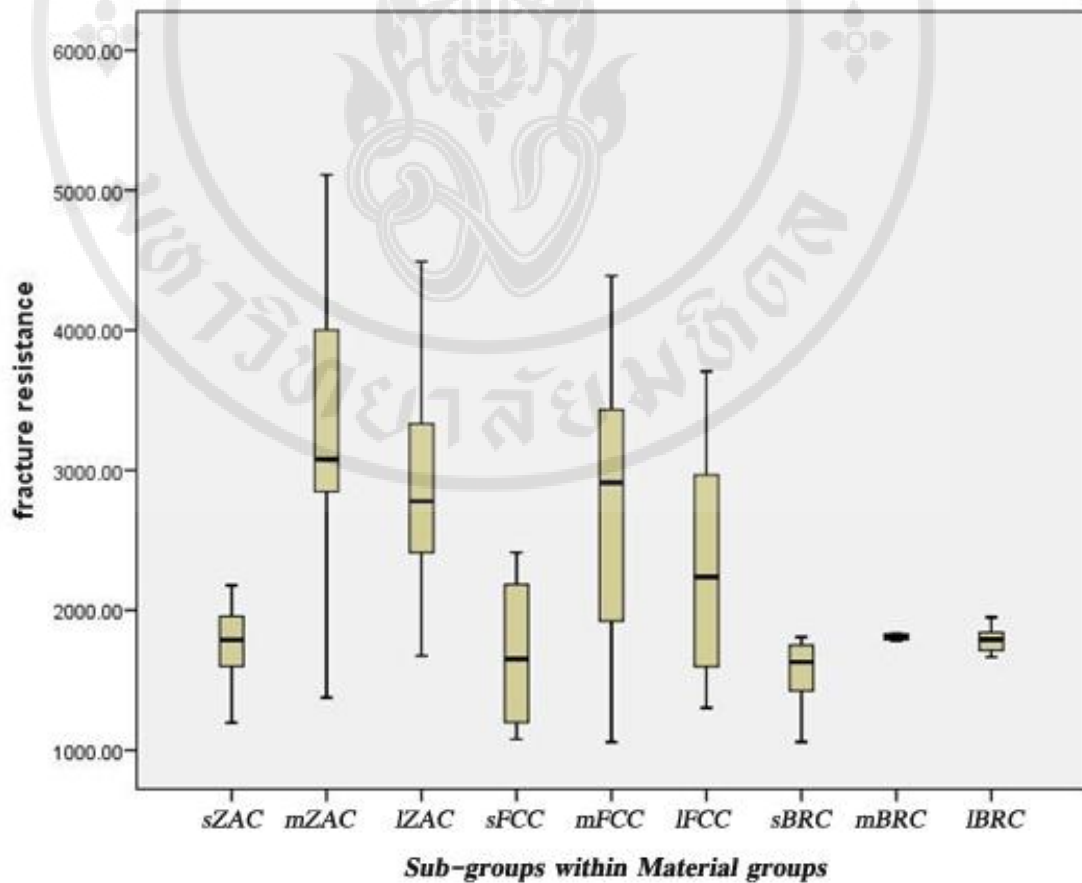


Fig 4-1: Boxplot of fracture resistance of crowns with different designs

* ZAC = Zirconia based All-Ceramic, FCC = Fusion with Crystal/Connect, BRC = Bonding with Resin Cement, s = Ø 4.5 mm, m = Ø 5.5 mm, l = Ø 6.5 mm

The means and standard deviations of fracture resistance after removing outliers are shown in table 4-3.

Table 4-3: Mean and standard deviation of fracture load (in Newton) of crowns with different designs after removing the outliers

Material types	Fracture resistance (N)		
	Ø 4.5 mm (s)	Ø 5.5 mm (m)	Ø 6.5 mm (l)
Zirconia based All-Ceramic (ZAC)	1787 ± 292	3295 ± 986	2851 ± 733
Fusion with Crystal/Connect (FCC)	1714 ± 508	2809 ± 1073	2293 ± 788
Bonding with Resin Cement (BRC)	1565 ± 229	1809 ± 22	1788 ± 93

Levene’s homogeneity of variance test found that the variances of each group were statistically different ($p < 0.05$). (Table 4-4)

Table 4-4: Levene's Test of Equality of Error Variances

Dependent Variable: fracture resistance

F	df1	df2	Sig.
6.556	8	92	.000

Two-way ANOVA test (Table 4-5) showed that there was significant interaction between the two main factors (abutment diameter and material types) as well as significant difference within each factor ($p < 0.05$), as shown in table 4-5.

Table 4-5: Analysis of variance

Dependent Variable: fracture resistance

Source	Sum of Squares	df	Mean Square	F	Sig.
Material	13658913.995	2	6829456.998	15.563	.000
Abutment	15151128.077	2	7575564.038	17.263	.000
material * abutment	4545414.677	4	1136353.669	2.589	.042
Error	40372916.217	92	438836.046		
Total	583894753.823	101			

*Statistical significant at $\alpha = 0.05$

The two main factors, abutment diameter and material types, were individual effect on fracture resistance. The estimated marginal means of fracture resistance were presented the interaction effect in fig 4-2 and fig 4-3.

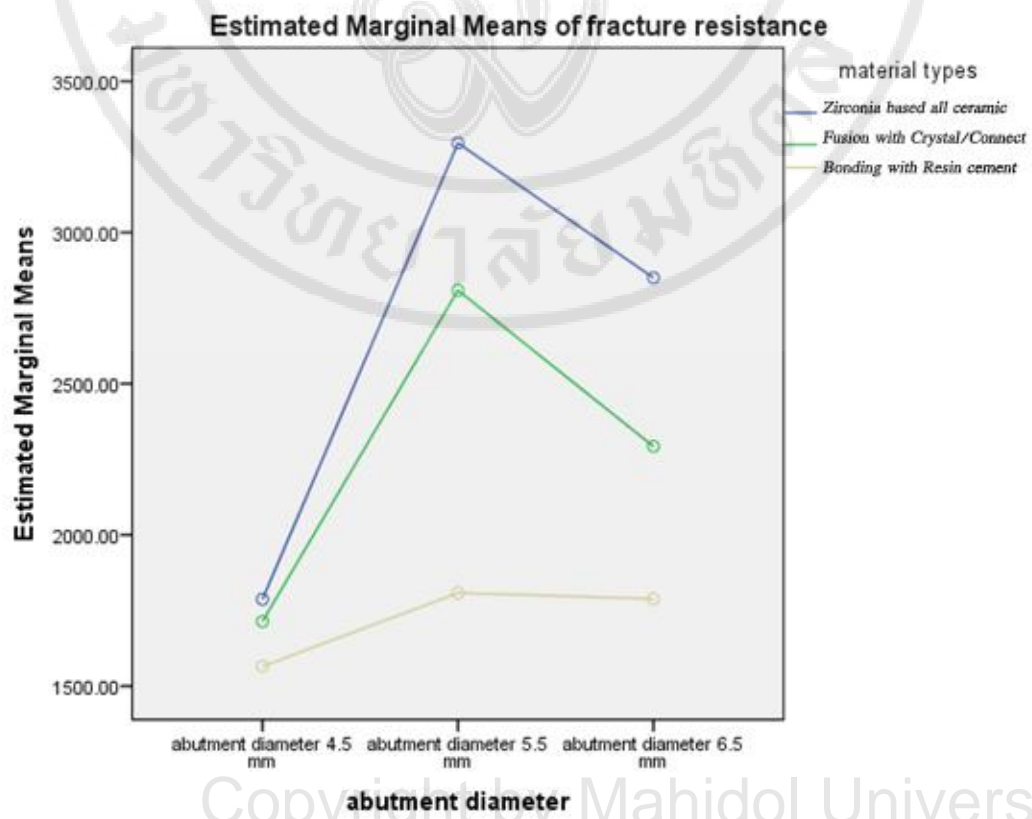


Fig. 4-2: Estimated marginal means of fracture resistance in 3 groups of material types

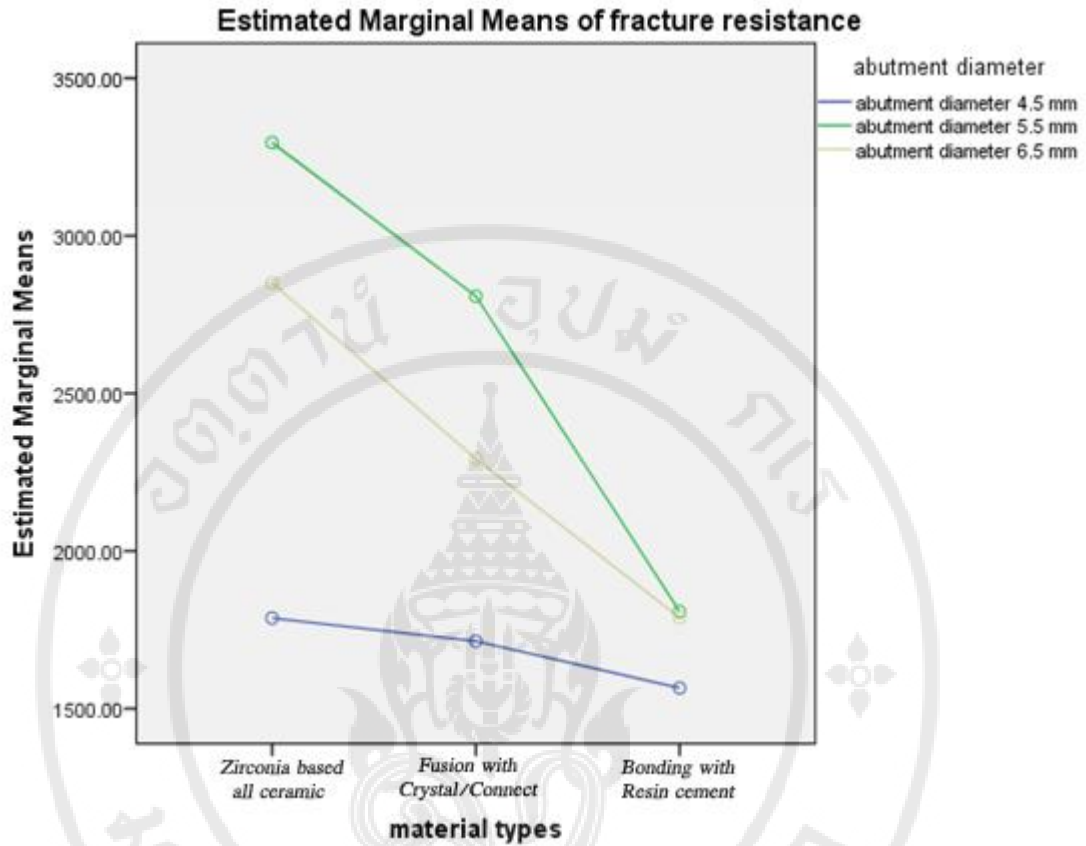


Fig. 4-3: Estimated marginal means of fracture resistance in 3 groups of abutment diameter

Tukey B test was used to analyze the effect within each factor. The fracture resistance in each group of material types was statistically significant, as well as the fracture resistance in each group of abutment diameter. (Table 4-6, Table 4-7)

Table 4-6: Tukey B Test of fracture resistance in each group of abutment diameter

		Fracture resistance (N)		
abutment diameter	N	Subset		
		1	2	3
abutment diameter 4.5 mm (s)	34	1683.0512		
abutment diameter 6.5 mm (l)	35		2325.5694	
abutment diameter 5.5 mm (m)	32			2741.1050

Table 4-7: Tukey B Test of fracture resistance in each group of material types

Fracture resistance (N)				
material types	N	Subset		
		1	2	3
Bonding with Resin cement (BRC)	31	1707.2371		
Fusion with Crystal/Connect (FCC)	36		2271.8411	
Zirconia based All-Ceramic (ZAC)	34			2694.8059

To estimate means of fracture resistance in material types of 3 groups, fracture resistance of control group (Zirconia based All-Ceramic) was the highest values. In test group, fracture resistance of test group A (Fusion with Crystal/Connect) was higher than fracture resistance of test group B (Bonding with Resin cement). There were significant differences in fracture resistance in 3 types of materials.

To compare means of fracture resistance in abutment diameter, fracture resistance of abutment diameter 5.5 was the highest values when compare with larger size of abutment (6.5 mm) and smaller size of abutment (4.5 mm). However, the largest size of abutment (6.5 mm) had the means of fracture resistance higher than the smallest size of abutment (4.5 mm). There were significant differences of fracture resistance of crowns in different sizes of abutment.

Observation of failure modes

All crowns were selected and fracture sites were inspected under visual observation, optical light microscope and scanning electron microscope (if necessary).

Mode of failure was classified in 3 categories:

- 1) Adhesive failure at framework and veneering interface
- 2) Cohesive failure within veneering layer
- 3) Combination of adhesive and cohesive failure

In control group (Zirconia based all ceramic - ZAC), failure mode were cohesive failure within veneering layer, shown in Fig. 4-4, except in sample number 5 and 7 of group ZAC. They were found combination of adhesive and cohesive failure.

In test group A (Fusion with Crystal/Connect - FCC), there were both types of failure mode. 24 samples of group FCC were found adhesive failure at framework and veneering interface (Fig. 4-5). And 12 samples of group FCC were found combination of adhesive and cohesive failure (Fig. 4-6). On the other hand, all samples in test group B (Bonding with Resin cement - BRC) were found adhesive failure at framework and veneering interface (Fig. 4-7).

Failure types in each group were shown in table 4-8.



Fig. 4-4: Cohesive failure within veneering layer (Control group - Zirconia based all ceramic)



Fig. 4-5: Adhesive failure at framework and veneering interface (Test group A - Fusion with Crystal/Connect)

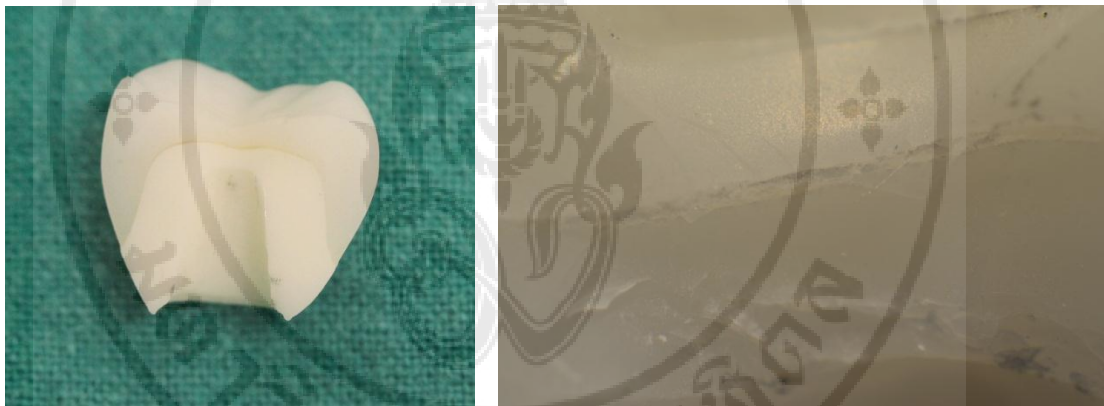


Fig. 4-6: Combination of adhesive and cohesive failure (Test group A - Fusion with Crystal/Connect)

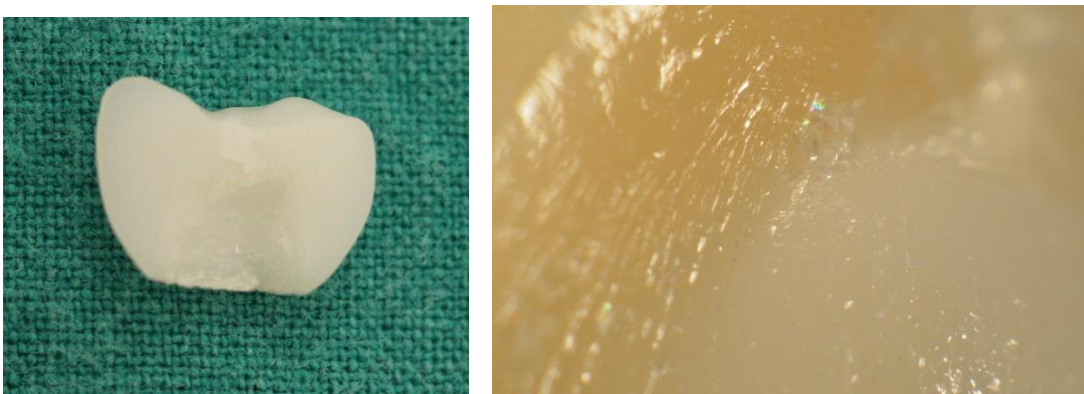


Fig. 4-7: Adhesive failure at framework and veneering interface (Test group B - Bonding with Resin cement)

Table 4-8: Mode of failure of crowns with different designs

Material types	Abutment diameter	Mode of failure (%)		
		Adhesive	Cohesive	Combination
Zirconia based All-Ceramic (ZAC)	4.5 mm (s)	-	100%	-
	5.5 mm (m)	-	100%	-
	6.5 mm (l)	-	83.33%	16.67%
Fusion with Crystal/Connect (FCC)	4.5 mm (s)	75%	-	25%
	5.5 mm (m)	58.33%	-	41.67%
	6.5 mm (l)	66.67%	-	33.33%
Bonding with Resin Cement (BRC)	4.5 mm (s)	100%	-	-
	5.5 mm (m)	100%	-	-
	6.5 mm (l)	100%	-	-

* **ZAC** = Zirconia based All-Ceramic, **FCC** = Fusion with Crystal/Connect, **BRC** = Bonding with Resin Cement, *s* = Ø 4.5 mm, *m* = Ø 5.5 mm, *l* = Ø 6.5 mm

CHAPTER V

DISCUSSION

All-ceramic crowns have been used popularly in both anterior and posterior area due to the esthetic property. However, the physical properties of all-ceramic crowns are weak and brittle.(43-47) To reinforce the fracture resistance of all-ceramic, zirconia has been used to fabricate the crown.(44) Some papers found that veneer chipping was the most common complication in veneered zirconia crown.(4, 48) The use of monolithic zirconia or lithium disilicate crown can reduce the incidence of veneer failure because of the superior mechanical properties than feldspathic ceramic.(49-51) Comparison between monolithic crown and bi-layered crown, the monolithic full anatomic design shows superior fracture resistance behavior compared with bi-layered crowns. The fracture load of full anatomic crown was almost double compared to that of the veneered ones, thus the stored strain energy at the moment of fracture was also almost double that of the veneered crown which would have assisted bifurcation of the fissure crack. Moreover, adhesive failure was found in bi-layered restorations. Some cracks propagated parallel to the interface with a thin layer of porcelain remained between the cracks and the interface.(41) However, full contour of zirconia material has effect to wear of the opposing teeth due to the hardness of zirconia. Some paper suggested using zirconia as the framework of bilayer all-ceramic crown.(44) Surface of feldspathic ceramic was roughen after using. That caused the exposure of the crystalline structure and increased the rates of natural tooth wear with time using.(52) To minimize abrasion of the natural opposing teeth and avoid initiation and progression of microcracks, smooth surface of ceramic was concerned by polishing and glazing.(53) Thus, lithium disilicate was appropriate restorative material to use as veneering layer on zirconia framework because mechanical properties of lithium disilicate were superior to those of feldspathic ceramic. It was approximately three times as strong as feldspathic ceramics.(49) Moreover, the CAD/CAM based fabrication of the veneer and attachment of the veneer to the

framework by use of different techniques have been proposed. The accuracy of CAD/CAM production can reduce hand-layered veneer defects from human error and increase the mechanical properties of the veneers.(54, 55) In this in vitro study, lithium disilicate with glazing surface was used as veneer on zirconia framework. Substructures of 3 different abutment sizes were controlled with same thickness in anatomical shape (occlusal thickness at central fossa = 0.5 mm). Various veneering layer of all crowns were controlled in standardized dimension from scanning model in the CAD process (mesio-distal width = 11.9 mm, bucco-lingual width = 11.1 mm, occlusal thickness at central fossa = 1.5 mm). The cement spaces (10-60 μm) were within the range of clinical acceptance.(56) There was no significant effect of variation of gap thickness.(57) The proper cement spaces in this in vitro study were 60 μm for framework gap and 40 μm for veneering gap. Moreover, In this study, fabrication of cobalt-chromium alloy by casting was used as replica abutment as well as the previous study. Nesse et al. reported that the milled group had better marginal fit than the cast group with no differences in seating within 2 groups.(58)

The aims of this study were to assess the fracture resistance and the mode of failure of the implant supported all ceramic zirconia-lithium disilicate crowns. It was reported that the biting force of healthy and young adults in the posterior region was approximately 597 N for female and 847 N for male with a maximum of about 900 N.(59, 60) Ferrario et al in 2004 reported an average posterior biting forces of 700N.(61) From the result of this study, the means of fracture resistance in 9 subgroups (>1,500N) were higher than the reported maximum of human biting force. However, the result might not represent the clinical situation for only a perpendicular force was applied. For better understanding of the fracture resistance of the tested materials, other impact factors, i.e. lateral force, thermocycling and emergency risks were expected to be taken into consideration.

The means of fracture load in the control group, Zirconia based All-Ceramic (1787 N - 3295 N), was the highest. The means of the fracture load in test group A, Fusion with Crystal/Connect (1714 N - 2809 N), was higher than fracture resistance of test group B, Bonding with Resin cement (1565 N - 1809 N). There were significant differences of fracture resistance in 3 types of materials. A recent in vitro study by Schmitter et al in 2014 investigating the effect on fracture resistance of the

technique to attach lithium disilicate veneer to zirconia frameworks also reported the higher value of fracture forces in fused veneer group (1388 ± 190 N) when compared to luted veneer group (1211 ± 158 N).⁽⁴²⁾ To compare the means of fracture resistance in abutment diameter, fracture resistance of group supported by abutment diameter 5.5 mm was the highest values (1809 N – 3295 N) when compared to those supported by larger size of abutment (6.5 mm) and by smaller size of abutment (4.5 mm). However, the group supported by the large size of abutment, 6.5 mm (1788 N – 2851 N), had the means of fracture resistance higher than those supported by the small size abutment, 4.5 mm (1565 – 1787). There were significant differences of fracture resistance of crowns in different sizes of the abutment. It might be explained that abutment size 5.5 mm was the most suitable design of crown thickness. Larger abutment size had an effect in fracture resistance due to the reduction of crown thickness. As well as, smaller abutment size could reduce the fracture resistance of restorative crowns due to less support of implant abutment. Furthermore, the abutment size 4.5 had the step at inner surface of zirconia substructure. This is the technical error in limitation of milling bur that need to be polishing before sintering. So it might lead the weak point in group of abutment size 4.5.

Concerning the mode of failure found in this study, the cohesive failure within veneering layer was mostly found in the control group (Zirconia based all ceramic). Kim et al reported that fractures in veneered layer were occurred in veneered zirconia crowns as a posterior implant-supported restoration that using the hand layer technique same as the control group in this study.⁽⁶²⁾ In a test group of this study, test group A (Fusion with Crystal/Connect) was found both types of failure modes, adhesive failure and combination failure. Whereas, test group B (Bonding with Resin cement) was found adhesive failure at framework and veneering interface. As well as the previous paper, a mixed failure mode was occurred with the fused crown and adhesive failure between the veneer and Multilink Implant cement was occurred in the luted crown.⁽⁴²⁾ Zahran et al. showed zirconia bi-layered crowns fractured in the veneering layer, as the cracks reached the interface and arrested, extended laterally parallel to the interface, with the core exposed.⁽⁶³⁾ Furthermore, spindle shaped voids, which were clearly evident under the central fossa, may be the crucial factor that

weakens the bi-layered composite and leads to adhesive failure.(41) It might be explained that the interface became weak point when the void defects were present.

In the present study, the lithium disilicate veneer layers were either cemented to zirconia core by either fusion technique (Fused with Crystal/Connect) or luting technique (Bonding with resin cement). The fracture resistance of group with fusion technique were superior to group with luting technique. It might be the negative effect that occurred at the initial point of the fracture at the interface between resin cement and ceramic. However, the fusion technique had too much cost due to additional specific material, Crystal/Connect and Ivomix, and some specimens revealed the catastrophic fracture from veneered layer to zirconia framework. On the other hand, the luting technique used available material, resin cement. In case of veneer fracture occurred with still intact zirconia substructure, it might be possible to repair those crowns with this technique.

The limitation in this in vitro study, the software (inLab 3D software) had limitation to construct the multilayer design technique with anatomical shape of substructure due to characteristic of implant abutment. So it needed to be constructed the substructure in each group of abutment size by manual. Furthermore, another human error was occurred while removing the large spur at outer surface of zirconia substructure. This might be increase the cement gap between substructure and veneering layer.

CHAPTER VI

CONCLUSION

Within limitations of this in vitro study the following conclusions can be made:

1. The mean fracture resistance of crowns fused with Crystal/Connect was significantly higher than that of crowns bonded with resin cement, but all the crowns have adequate fracture resistance to be used as implant supported restorations in posterior region.
2. There were significant differences of fracture resistance of crowns in different sizes of abutment. The suitable size of abutment was abutment diameter 5.5 mm because it had the highest value of fracture resistance.

REFERENCES

1. Buser D, Janner SF, Wittneben JG, Bragger U, Ramseier CA, Salvi GE. 10-year survival and success rates of 511 titanium implants with a sandblasted and acid-etched surface: a retrospective study in 303 partially edentulous patients. *Clinical implant dentistry and related research*. 2012 Dec;14(6):839-51. PubMed PMID: 22897683.
2. Pjetursson BE, Bragger U, Lang NP, Zwahlen M. Comparison of survival and complication rates of tooth-supported fixed dental prostheses (FDPs) and implant-supported FDPs and single crowns (SCs). *Clinical oral implants research*. 2007 Jun;18 Suppl 3:97-113. PubMed PMID: 17594374.
3. Wittneben JG, Buser D, Salvi GE, Burgin W, Hicklin S, Bragger U. Complication and failure rates with implant-supported fixed dental prostheses and single crowns: a 10-year retrospective study. *Clinical implant dentistry and related research*. 2014 Jun;16(3):356-64. PubMed PMID: 23551688.
4. Al-Amleh B, Lyons K, Swain M. Clinical trials in zirconia: a systematic review. *J Oral Rehabil*. 2010 Aug;37(8):641-52. PubMed PMID: 20406352.
5. Denry I, Kelly JR. State of the art of zirconia for dental applications. *Dental materials : official publication of the Academy of Dental Materials*. 2008 Mar;24(3):299-307. PubMed PMID: 17659331.
6. Gomes AL, Montero J. Zirconia implant abutments: a review. *Medicina oral, patologia oral y cirugia bucal*. 2011 Jan;16(1):e50-5. PubMed PMID: 20526253.
7. Sailer I, Philipp A, Zembic A, Pjetursson BE, Hammerle CH, Zwahlen M. A systematic review of the performance of ceramic and metal implant abutments supporting fixed implant reconstructions. *Clinical oral implants research*. 2009 Sep;20 Suppl 4:4-31. PubMed PMID: 19663946.

8. Mitov G, Heintze SD, Walz S, Woll K, Muecklich F, Pospiech P. Wear behavior of dental Y-TZP ceramic against natural enamel after different finishing procedures. *Dental materials : official publication of the Academy of Dental Materials*. 2012 Aug;28(8):909-18. PubMed PMID: 22608163.
9. Miyazaki T, Nakamura T, Matsumura H, Ban S, Kobayashi T. Current status of zirconia restoration. *Journal of prosthodontic research*. 2013 Oct;57(4):236-61. PubMed PMID: 24140561.
10. Stimmelmayer M, Sagerer S, Erdelt K, Beuer F. In vitro fatigue and fracture strength testing of one-piece zirconia implant abutments and zirconia implant abutments connected to titanium cores. *The International journal of oral & maxillofacial implants*. 2013 Mar-Apr;28(2):488-93. PubMed PMID: 23527351.
11. Raghavan RN. *Ceramics in Dentistry, Sintering of Ceramics - New Emerging Techniques 2012*. Available from: <http://www.intechopen.com/books/sintering-of-ceramics-new-emerging-techniques/ceramics-in-dentistry>.
12. El-Meliegy E, Noort Rv. *Glasses and Glass Ceramics for Medical Applications*: Springer New York; 2012.
13. Stookey D. Catalyzed crystallization of glasses in theory and practice. *Ind Eng Chem*. 1959 July 1959;51(7):805-8.
14. Beall G. Structure, properties, and nucleation of glass - ceramics. In: Hench L, Freiman S, editors. *Advances in Nucleation and Crystallization in Glasses*. Special Publ. No. 5 ed: The American Ceramic Society, Columbus, OH; 1971. p. 251 - 61.
15. Freiman SW, Hench LL. Effect of Crystallization on the Mechanical Properties of Li₂O-SiO₂ Glass-Ceramics. *Journal of the American Ceramic Society*. 1972;55(2):86-90.
16. Hannon AC, Vessal B, Parker JM. The structure of alkali silicate glasses. *Journal of Non-Crystalline Solids*. 1992 11/2;150(1-3):97-102.
17. Soares Jr PC, Zanotto ED, Fokin VM, Jain H. TEM and XRD study of early crystallization of lithium disilicate glasses. *Journal of Non-Crystalline Solids*. 2003 12/1;331(1-3):217-27.

18. Holand W, Schweiger M, Frank M, Rheinberger V. A comparison of the microstructure and properties of the IPS Empress 2 and the IPS Empress glass-ceramics. *Journal of biomedical materials research*. 2000;53(4):297-303. PubMed PMID: 10898870. Epub 2000/07/18. eng.
19. Holland W, Beall G. *Glass-ceramic technology*. The American Ceramic Society, Westerville, OH, USA2002. Available from: <http://dx.doi.org/10.2298/SOS0403216U>.
20. Holand W, Apel E, van't Hoen C, Rheinberger V. Studies of crystal phase formations in high-strength lithium disilicate glass-ceramics. *J Non-Cryst Solid*. 2006;72(81):4041-50. .
21. Tashiro T, Wada M. *Glass-ceramics crystallized with zirconia*. *Advances in Glass Technology*. Plenum Press, New York1963. p. 18-9.
22. Apel E, van't Hoen C, Rheinberger V, Höland W. Influence of ZrO₂ on the crystallization and properties of lithium disilicate glass-ceramics derived from a multi-component system. *Journal of the European Ceramic Society*. 2007 //;27(2-3):1571-7.
23. Griggs JA. Recent advances in materials for all-ceramic restorations. *Dental clinics of North America*. 2007 Jul;51(3):713-27, viii. PubMed PMID: 17586152. Pubmed Central PMCID: 2833171.
24. Tinschert J, Zvez D, Marx R, Anusavice KJ. Structural reliability of alumina-, feldspar-, leucite-, mica- and zirconia-based ceramics. *Journal of dentistry*. 2000 Sep;28(7):529-35. PubMed PMID: 10960757.
25. Sulaiman F, Chai J, Jameson LM, Wozniak WT. A comparison of the marginal fit of In-Ceram, IPS Empress, and Procera crowns. *The International journal of prosthodontics*. 1997 Sep-Oct;10(5):478-84. PubMed PMID: 9495168.
26. Yeo IS, Yang JH, Lee JB. In vitro marginal fit of three all-ceramic crown systems. *The Journal of prosthetic dentistry*. 2003 Nov;90(5):459-64. PubMed PMID: 14586310.
27. Sundh A, Sjogren G. Fracture resistance of all-ceramic zirconia bridges with differing phase stabilizers and quality of sintering. *Dental materials : official publication of the Academy of Dental Materials*. 2006 Aug;22(8):778-84. PubMed PMID: 16414111.

28. Helvey G. Monolithic versus bilayered restorations: a closer look. *VISTAS-Dawson*. 2010 July/August 3(2).
29. Ozcan M. Fracture reasons in ceramic-fused-to-metal restorations. *J Oral Rehabil*. 2003 Mar;30(3):265-9. PubMed PMID: 12588498.
30. Imbeni V, Kruzic JJ, Marshall GW, Marshall SJ, Ritchie RO. The dentin-enamel junction and the fracture of human teeth. *Nature materials*. 2005 Mar;4(3):229-32. PubMed PMID: 15711554. Epub 2005/02/16. eng.
31. Spear F, Holloway J. Which all-ceramic system is optimal for anterior esthetics? *Journal of the American Dental Association (1939)*. 2008 Sep;139 Suppl:19S-24S. PubMed PMID: 18768905. Epub 2008/09/26. eng.
32. Sun T, Zhou S, Lai R, Liu R, Ma S, Zhou Z, et al. Load-bearing capacity and the recommended thickness of dental monolithic zirconia single crowns. *Journal of the mechanical behavior of biomedical materials*. 2014 Jul;35:93-101. PubMed PMID: 24762856.
33. Zhang Y, Lee JJ, Srikanth R, Lawn BR. Edge chipping and flexural resistance of monolithic ceramics. *Dental materials : official publication of the Academy of Dental Materials*. 2013 Dec;29(12):1201-8. PubMed PMID: 24139756. Pubmed Central PMCID: 4000448.
34. Dundar M, Ozcan M, Gokce B, Comlekoglu E, Leite F, Valandro LF. Comparison of two bond strength testing methodologies for bilayered all-ceramics. *Dental materials : official publication of the Academy of Dental Materials*. 2007 May;23(5):630-6. PubMed PMID: 16844212.
35. Stappert CF, Guess PC, Chitmongkolsuk S, Gerds T, Strub JR. Partial coverage restoration systems on molars--comparison of failure load after exposure to a mastication simulator. *J Oral Rehabil*. 2006 Sep;33(9):698-705. PubMed PMID: 16922744. Epub 2006/08/23. eng.
36. Silva NR, Bonfante EA, Martins LM, Valverde GB, Thompson VP, Ferencz JL, et al. Reliability of reduced-thickness and thinly veneered lithium disilicate crowns. *Journal of dental research*. 2012 Mar;91(3):305-10. PubMed PMID: 22205635. Pubmed Central PMCID: 3275335.

37. Wang RR, Lu CL, Wang G, Zhang DS. Influence of cyclic loading on the fracture toughness and load bearing capacities of all-ceramic crowns. *International journal of oral science*. 2014 Jun;6(2):99-104. PubMed PMID: 24335786.
38. Zhao K, Pan Y, Guess PC, Zhang XP, Swain MV. Influence of veneer application on fracture behavior of lithium-disilicate-based ceramic crowns. *Dental materials : official publication of the Academy of Dental Materials*. 2012 Jun;28(6):653-60. PubMed PMID: 22456006.
39. Dhima M, Assad DA, Volz JE, An KN, Berglund LJ, Carr AB, et al. Evaluation of fracture resistance in aqueous environment of four restorative systems for posterior applications. Part 1. *Journal of prosthodontics : official journal of the American College of Prosthodontists*. 2013 Jun;22(4):256-60. PubMed PMID: 23279080.
40. Korber KH, Ludwig K, Dunner P. [Experimental studies of the abrasion effect between dental enamel and dental ceramic]. *Deutsche zahnärztliche Zeitschrift*. 1984 Jan;39(1):2-11. PubMed PMID: 6584299. Epub 1984/01/01. Experimentelle Untersuchungen zur Abrasionswirkung zwischen Zahnschmelz und Dentalkeramik. ger.
41. Zhao K, Wei YR, Pan Y, Zhang XP, Swain MV, Guess PC. Influence of veneer and cyclic loading on failure behavior of lithium disilicate glass-ceramic molar crowns. *Dental materials : official publication of the Academy of Dental Materials*. 2014 Feb;30(2):164-71. PubMed PMID: 24331550.
42. Schmitter M, Schweiger M, Mueller D, Rues S. Effect on in vitro fracture resistance of the technique used to attach lithium disilicate ceramic veneer to zirconia frameworks. *Dental materials : official publication of the Academy of Dental Materials*. 2014 Feb;30(2):122-30. PubMed PMID: 24246472. Epub 2013/11/20. eng.
43. Deany IL. Recent advances in ceramics for dentistry. *Critical reviews in oral biology and medicine : an official publication of the American Association of Oral Biologists*. 1996;7(2):134-43. PubMed PMID: 8875028.

44. Tsalouchou E, Cattell MJ, Knowles JC, Pittayachawan P, McDonald A. Fatigue and fracture properties of yttria partially stabilized zirconia crown systems. *Dental materials : official publication of the Academy of Dental Materials*. 2008 Mar;24(3):308-18. PubMed PMID: 17681371.
45. Kelly JR. Dental ceramics: what is this stuff anyway? *Journal of the American Dental Association (1939)*. 2008 Sep;139 Suppl:4S-7S. PubMed PMID: 18768902.
46. Heintze SD, Rousson V. Fracture rates of IPS Empress all-ceramic crowns--a systematic review. *The International journal of prosthodontics*. 2010 Mar-Apr;23(2):129-33. PubMed PMID: 20305850.
47. Sobrinho LC, Cattell MJ, Knowles JC. Fracture strength of all-ceramic crowns. *Journal of materials science Materials in medicine*. 1998 Oct;9(10):555-9. PubMed PMID: 15348687.
48. Triwatana P, Nagaviroj N, Tulapornchai C. Clinical performance and failures of zirconia-based fixed partial dentures: a review literature. *The journal of advanced prosthodontics*. 2012 May;4(2):76-83. PubMed PMID: 22737311. Pubmed Central PMCID: 3381206.
49. Baltzer A. All-ceramic single-tooth restorations: choosing the material to match the preparation--preparing the tooth to match the material. *International journal of computerized dentistry*. 2008;11(3-4):241-56. PubMed PMID: 19216315.
50. Kern M, Sasse M, Wolfart S. Ten-year outcome of three-unit fixed dental prostheses made from monolithic lithium disilicate ceramic. *Journal of the American Dental Association (1939)*. 2012 Mar;143(3):234-40. PubMed PMID: 22383203.
51. Stawarczyk B, Ozcan M, Schmutz F, Trottmann A, Roos M, Hammerle CH. Two-body wear of monolithic, veneered and glazed zirconia and their corresponding enamel antagonists. *Acta odontologica Scandinavica*. 2013 Jan;71(1):102-12. PubMed PMID: 22364372.

52. Esquivel-Upshaw J, Rose W, Oliveira E, Yang M, Clark AE, Anusavice K. Randomized, controlled clinical trial of bilayer ceramic and metal-ceramic crown performance. *Journal of prosthodontics : official journal of the American College of Prosthodontists*. 2013 Apr;22(3):166-73. PubMed PMID: 22978697. Pubmed Central PMCID: 3625457.
53. Hmaidouch R, Weigl P. Tooth wear against ceramic crowns in posterior region: a systematic literature review. *International journal of oral science*. 2013 Dec;5(4):183-90. PubMed PMID: 24136675. Pubmed Central PMCID: 3967317.
54. Beuer F, Schweiger J, Eichberger M, Kappert HF, Gernet W, Edelhoff D. High-strength CAD/CAM-fabricated veneering material sintered to zirconia copings--a new fabrication mode for all-ceramic restorations. *Dental materials : official publication of the Academy of Dental Materials*. 2009 Jan;25(1):121-8. PubMed PMID: 18620748.
55. Schmitter M, Mueller D, Rues S. Chipping behaviour of all-ceramic crowns with zirconia framework and CAD/CAM manufactured veneer. *Journal of dentistry*. 2012 Feb;40(2):154-62. PubMed PMID: 22197634.
56. Iwai T, Komine F, Kobayashi K, Saito A, Matsumura H. Influence of convergence angle and cement space on adaptation of zirconium dioxide ceramic copings. *Acta odontologica Scandinavica*. 2008 Aug;66(4):214-8. PubMed PMID: 18607834. Epub 2008/07/09. eng.
57. Rosentritt M, Steiger D, Behr M, Handel G, Kolbeck C. Influence of substructure design and spacer settings on the in vitro performance of molar zirconia crowns. *Journal of dentistry*. 2009 Dec;37(12):978-83. PubMed PMID: 19695301. Epub 2009/08/22. eng.
58. Nesse H, Ulstein DM, Vaage MM, Oilo M. Internal and marginal fit of cobalt-chromium fixed dental prostheses fabricated with 3 different techniques. *The Journal of prosthetic dentistry*. 2015 Nov;114(5):686-92. PubMed PMID: 26213267. Epub 2015/07/28. eng.

59. Waltimo A, Kononen M. Maximal bite force and its association with signs and symptoms of craniomandibular disorders in young Finnish non-patients. *Acta odontologica Scandinavica*. 1995 Aug;53(4):254-8. PubMed PMID: 7484109.
60. Waltimo A, Nystrom M, Kononen M. Bite force and dentofacial morphology in men with severe dental attrition. *Scandinavian journal of dental research*. 1994 Apr;102(2):92-6. PubMed PMID: 8016561.
61. Ferrario VF, Sforza C, Zanotti G, Tartaglia GM. Maximal bite forces in healthy young adults as predicted by surface electromyography. *Journal of dentistry*. 2004 Aug;32(6):451-7. PubMed PMID: 15240063.
62. Kim JH, Lee SJ, Park JS, Ryu JJ. Fracture load of monolithic CAD/CAM lithium disilicate ceramic crowns and veneered zirconia crowns as a posterior implant restoration. *Implant dentistry*. 2013 Feb;22(1):66-70. PubMed PMID: 23296031.
63. Zahran M, El-Mowafy O, Tam L, Watson PA, Finer Y. Fracture strength and fatigue resistance of all-ceramic molar crowns manufactured with CAD/CAM technology. *Journal of prosthodontics : official journal of the American College of Prosthodontists*. 2008 Jul;17(5):370-7. PubMed PMID: 18355164.



Table 1: Normality test for fracture resistance of crowns (n = 12)

		Kolmogorov-Smirnov ^a			Shapiro-Wilk		
		Statistic	Df	Sig.	Statistic	df	Sig.
Fracture resistance	sZAC	.194	12	.200*	.910	12	.214
	mZAC	.194	12	.200*	.950	12	.635
	IZAC	.144	12	.200*	.960	12	.786
	sFCC	.178	12	.200*	.888	12	.110
	mFCC	.158	12	.200*	.949	12	.625
	IFCC	.219	12	.115	.913	12	.230
	sBRC	.158	12	.200*	.911	12	.220
	mBRC	.276	12	.012	.844	12	.031
	IBRC	.207	12	.167	.786	12	.007

*. This is a lower bound of the true significance.

a. Lilliefors Significance Correction

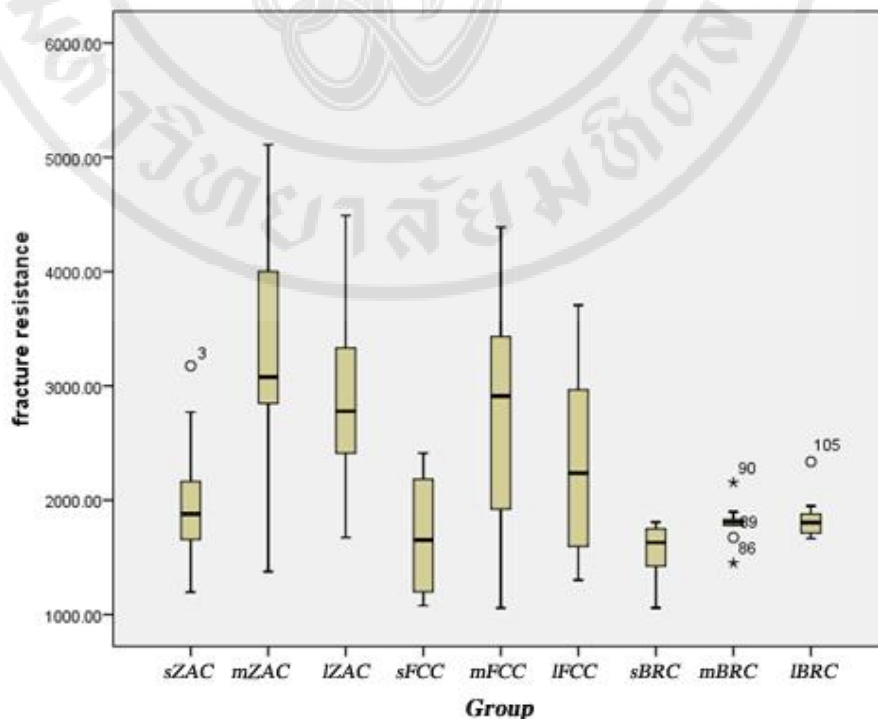


Fig. 1: Boxplot of fracture resistance in each group

Table 2: Normality test for fracture resistance after removing outliers (1st cut)

		Kolmogorov-Smirnov ^a			Shapiro-Wilk		
		Statistic	Df	Sig.	Statistic	df	Sig.
Fracture resistance	sZAC	.150	11	.200*	.948	11	.620
	mZAC	.194	12	.200*	.950	12	.635
	IZAC	.144	12	.200*	.960	12	.786
	sFCC	.178	12	.200*	.888	12	.110
	mFCC	.158	12	.200*	.949	12	.625
	IFCC	.219	12	.115	.913	12	.230
	sBRC	.158	12	.200*	.911	12	.220
	mBRC	.243	10	.098	.890	10	.171
	IBRC	.127	11	.200*	.963	11	.807

*. This is a lower bound of the true significance.

a. Lilliefors Significance Correction

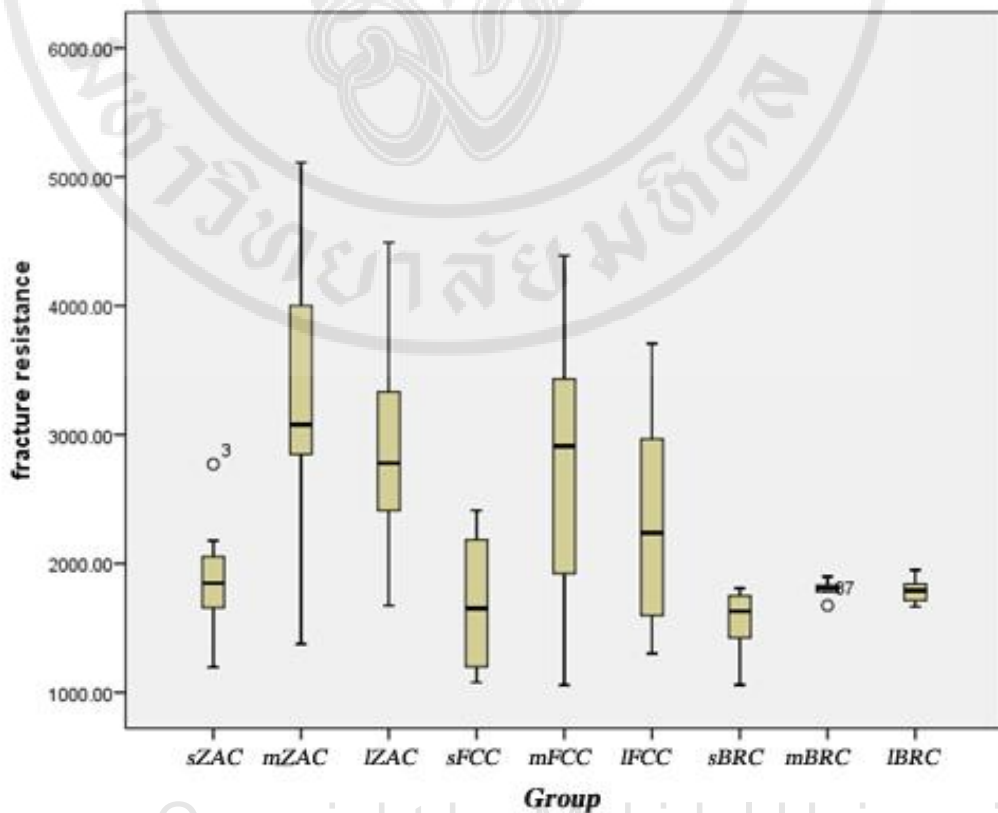


Fig. 2: Boxplot of fracture resistance in each group

Table 3: Normality test for fracture resistance after removing outliers (2nd cut)

		Kolmogorov-Smirnov ^a			Shapiro-Wilk		
		Statistic	Df	Sig.	Statistic	df	Sig.
Fracture resistance	sZAC	.150	10	.200*	.951	10	.684
	mZAC	.194	12	.200*	.950	12	.635
	IZAC	.144	12	.200*	.960	12	.786
	sFCC	.178	12	.200*	.888	12	.110
	mFCC	.158	12	.200*	.949	12	.625
	IFCC	.219	12	.115	.913	12	.230
	sBRC	.158	12	.200*	.911	12	.220
	mBRC	.234	9	.170	.869	9	.119
	IBRC	.127	11	.200*	.963	11	.807

*. This is a lower bound of the true significance.

a. Lilliefors Significance Correction

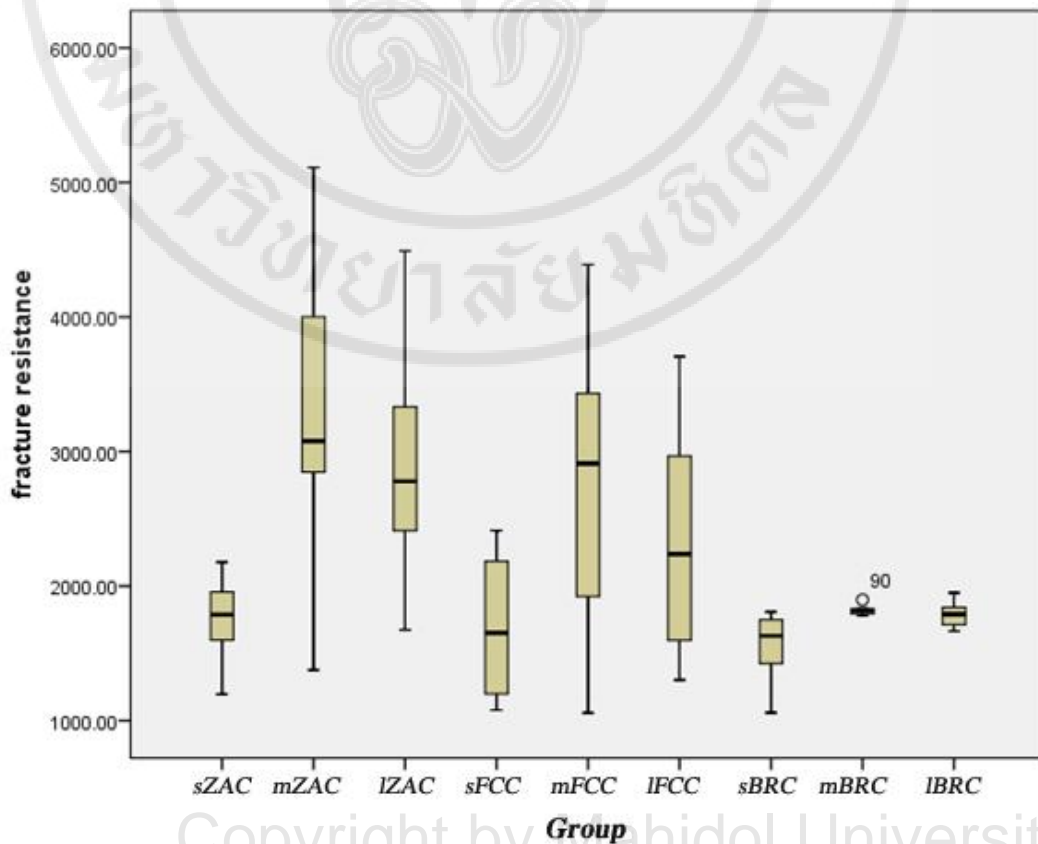


Fig. 3: Boxplot of fracture resistance in each group

Table 4: Normality test for fracture resistance after removing outliers (3rd cut)

		Kolmogorov-Smirnov ^a			Shapiro-Wilk		
		Statistic	Df	Sig.	Statistic	df	Sig.
Fracture resistance	sZAC	.150	10	.200*	.951	10	.684
	mZAC	.194	12	.200*	.950	12	.635
	IZAC	.144	12	.200*	.960	12	.786
	sFCC	.178	12	.200*	.888	12	.110
	mFCC	.158	12	.200*	.949	12	.625
	IFCC	.219	12	.115	.913	12	.230
	sBRC	.158	12	.200*	.911	12	.220
	mBRC	.179	8	.200*	.874	8	.165
	IBRC	.127	11	.200*	.963	11	.807

*. This is a lower bound of the true significance.

a. Lilliefors Significance Correction

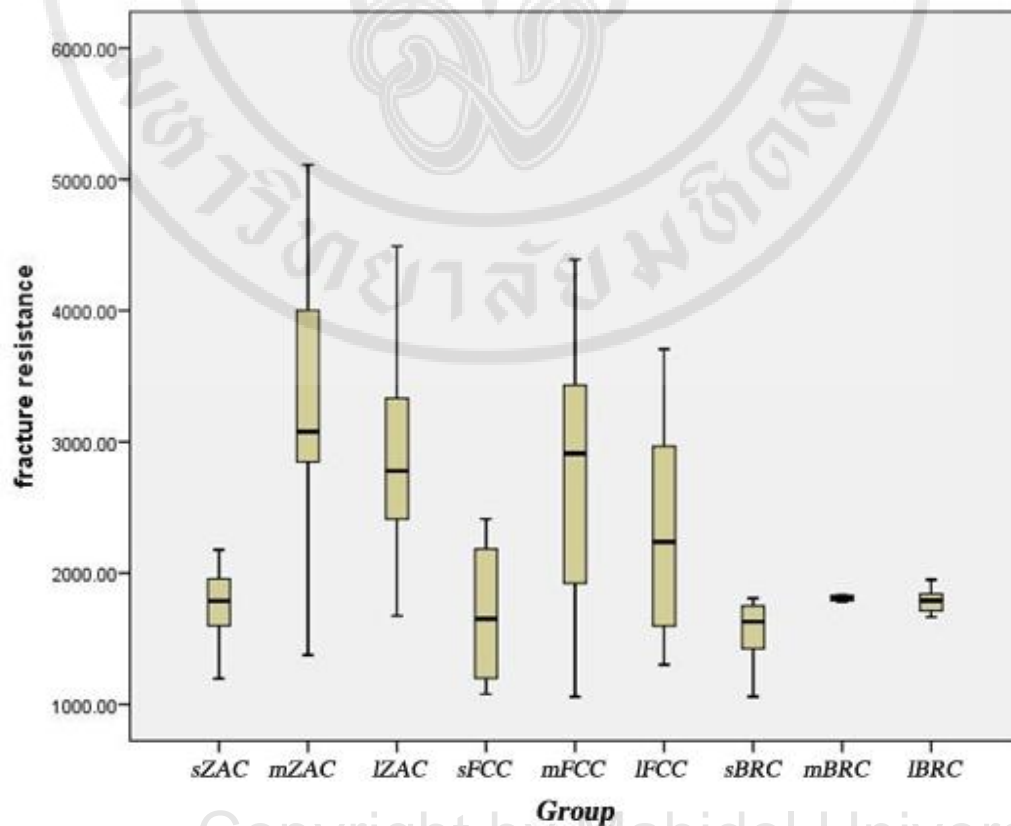


Fig. 4: Boxplot of fracture resistance in each group

BIOGRAPHY

NAME	Nattanich Bunyasresth
DATE OF BIRTH	3 November 1985
PLACE OF BIRTH	Bangkok, Thailand
INSTITUTIONS ATTENDED	Chulalongkorn University (2004-2009) Doctor of Dental Surgery Mahidol University (2013-2015) Master of Science (Dentistry)
HOME ADDRESS	79 Pattawikorn Soi Nawamin 70 yak 3-10 Nawamin Rd. Klongkum Bungkum Bangkok Thailand 10240 Tel. (+668) 0248-3334 E-mail: ppdeinfi@hotmail.com
EMPLOYMENT ADDRESS	Faculty of Dentistry, Mahidol University Yothi Rd., Rachathewi Bangkok Thailand 10400